RESEARCH REPORT

NAC1 directs CEP1-CEP3 peptidase expression and decreases cell wall extensins linked to root hair growth in Arabidopsis

Diana R. Rodríguez-García[1], Eliana Marzol[1], Yossmayer del Carmen Rondón Guerrero[1], Lucía Ferrero[2], Andrés Hugo Rossi[1], Esteban A. Miglietta[1], Ariel. A. Aptekmann[3,4], Javier Martínez Pacheco[1], Mariana Carignani[1], Victoria Berdión Gabarain[1], Leonel E. Lopez[1], Gabriela Diaz Dominguez[1], José Juan Sánchez-Serrano[6], Lin Xu[5], Alejandro D. Nadra[3,4], Federico Ariel[2], Enrique Rojo[6], José M. Estevez[1,7,8,9,†]

[1]Fundación Instituto Leloir and IIBBA-CONICET. Av. Patricias Argentinas 435, Buenos Aires C1405BWE, Argentina.

[2]Instituto de Agrobiotecnología del Litoral, CONICET, Universidad Nacional del Litoral, Colectora Ruta Nacional 168 km 0, 3000, Santa Fe, Argentina.

[3]Departamento de Fisiología, Biología Molecular y Celular, Instituto de Biociencias, Biotecnología y Biología Traslacional (iB3). Facultad de Ciencias Exactas y Naturales, Universidad de Buenos Aires, Ciudad Universitaria, Buenos Aires C1428EGA, Argentina.

[4]Departamento de Química Biológica, Facultad de Ciencias Exactas y Naturales, Universidad de Buenos Aires (IQUIBICEN-CONICET), Ciudad Universitaria, Buenos Aires C1428EGA, Argentina.

[5]National Laboratory of Plant Molecular Genetics, CAS Center for Excellence in Molecular Plant Sciences, Institute of Plant Physiology and Ecology, Shanghai Institutes for Biological Sciences, Chinese Academy of Sciences, Shanghai 200032, China

[6]Centro Nacional de Biotecnología, Consejo Superior de Investigaciones Científicas, Cantoblanco, E-28049 Madrid, Spain

[7]Centro de Biotecnología Vegetal, Facultad de Ciencias de la Vida, Universidad Andrés Bello and Millennium Institute for Integrative Biology (iBio), Santiago, Chile

[8]ANID – Millennium Institute for Integrative Biology (iBio), 7500000 Santiago, Chile

[9]ANID –Millennium Nucleus for the Development of Super Adaptable Plants (MN-SAP), 8331150 Santiago, Chile

[†] Correspondence should be addressed. Email: jestevez@leloir.org.ar (J.M.E).

Word count: x,xxx

Running Head: AtCEP1-AtCEP3 negatively modulate root hair growth.

Author for Correspondence:

José M. Estevez

Fundación Instituto Leloir, Av. Patricias Argentinas 435, Buenos Aires C1405BWE, Argentina.
TE: 54-115238-7500 EXT. 3206

Centro de Biotecnología Vegetal, Facultad de Ciencias de la Vida, Universidad Andrés Bello and Millennium Institute for Integrative Biology (iBio), Santiago CP 8370146, Chile.

Email: jestevez@leloir.org.ar / jose.estevez@unab.cl

Special Issue: Plant cell walls

Abstract Word count: 265

Text Word count: 2,739

Figures 4

Figure S1-S7

Tables S1-S3

References: 48

Abstract

Plant genomes encode a unique group of papain-type Cysteine EndoPeptidases (CysEPs) containing a KDEL endoplasmic reticulum (ER) retention signal (KDEL-CysEPs or CEPs). CEPs process the cell-wall scaffolding EXTENSIN proteins (EXTs), which regulate *de novo* cell wall formation and cell expansion. Since CEPs are able to cleave EXTs and EXT-related proteins, acting as cell wall-weakening agents, they may play a role in cell elongation. *Arabidopsis thaliana* genome encodes three CEPs (AtCPE1-AtCEP3). Here we report that the three Arabidopsis CEPs, *AtCEP1-AtCEP,* are highly expressed in root-hair cell files. Single mutants have no evident root-hair phenotype, but *atcep1-3 atcep3-2* and *atcep1-3 atcep2-2* double mutants have longer root hairs (RHs) than wild type (Wt) plants, suggesting that expression of *AtCEPs* in root trichoblasts restrains polar elongation of the RH. We provide evidence that the transcription factor *NAC1* activates AtCEPs expression in roots to limit RH length. Chromatin immunoprecipitation indicates that NAC1 binds the promoter of *AtCEP2* and may directly regulate its expression. Indeed, Inducible *NAC1* overexpression increases *AtCEP1 and AtCEP2* transcript levels in roots and leads to reduced RH growth while the loss of function *nac1-2* mutation reduces *AtCEP1-AtCEP3* gene expression and enhances RH growth. Likewise, expression of a dominant chimeric NAC1-SRDX repressor construct leads to increased RH length. Finally, we show that RH cell walls in the *atcep1-1 atcep3-2* double mutant have reduced levels of EXT secretion/insolubilization, suggesting that the defects in RH elongation are linked to alterations in EXT processing and accumulation. Taken together, our results support the involvement of the NAC1-AtCEP regulatory module in controlling RH polar growth through EXT processing and insolubilization at the cell wall.

.

Introduction

In plants there is a unique group of papain-type Cysteine EndoPeptidases (CysEPs) containing a KDEL endoplasmic reticulum (ER) retention signal (KDEL-CysEPs or CEPs) for which no homologous genes have been identified in mammals or yeast (Gietl et al. 2000). CEPs are synthesized as pre-pro-enzyme and co-translationally translocated into the ER, where the pre-sequence is removed and the pro-enzyme is finally released from the ricinosomes (ER-associated structures) upon vacuolar collapse and acidification of the cytosol, triggering the maturation of the enzyme (Schmid et al. 1999, 2001; Beers et al. 2000; Zhang et al. 2014). AtCEP1 (At5g50260), AtCEP2 (At3g48340), and AtCEP3 (At3g48350) are three *Arabidopsis thaliana* AtCEPs with broad expression patterns in vegetative and reproductive tissues along the plant, including root tissues (Helm et al. 2008; Hierl et al. 2014; Zhou et al. 2016). Several CEPs have been identified in cells or tissues associated with programmed cell death (PCD), where they play crucial roles in intracellular protein degradation (Tanaka 1991; Becker et al. 1997; He and Kermode 2003; Zhang et al. 2014; Olvera-Carrillo Y et al 2015; Chen et al. 2016). AtCEP1 was found to be a central mediator of tapetal PCD, allowing tapetal cell degeneration and functional pollen formation (Zhang et al. 2014). In addition, AtCEP1 and AtCEP2 in Arabidopsis were found to be functional in the *de novo* emergence of adventitious root tips associated with EXT-degradation and regulated by the NAC1 transcription factor (Chen et al. 2016). More recently, it was reported that *AtCEP1* and *AtCEP2* are expressed in root epidermal cells that separate to allow LR emergence, and that loss of function of *AtCEP1* or *AtCEP2* causes delayed emergence of LR primordia, suggesting that these KDEL-CysEPs might be involved in cell-wall remodelling for cell separation during development (Howing et al. 2018).

In addition to the papain-type preference for neutral amino acids with large aliphatic and non-polar (Leu, Val, Met) or aromatic (Phe, Tyr, Trp) side chains in the P2 position, Ricinus CEP (RcCysEP) exhibits an unusually broad substrate specificity. This broad substrate specificity is a result of the active site cleft of KDEL-CysEPs, which accepts a wide variety of amino acids, including proline and the glycosylated hydroxyproline of hydroxyproline-rich glycoproteins (HRGP) of the cell wall (Than et al. 2004). The amino acid residues that are essential for this generally more open structure of the active site cleft, as well as those that define the catalytic pocket, are highly conserved among known KDEL-CysEPs (Hierl et al. 2014). It can recognize the Ser-$(Hyp)_{3-5}$ repeats, *O*-glycosylated Hyp, and prolines at one-two amino acids relative to the cleavage site (Than et al., 2004; Helm et al. 2008; Hierl et al. 2014). These Ser-$(Hyp)_{3-5}$ repeats with *O*-glycosylated modifications are frequently observed in structural *O*-glycoproteins Extensins (EXTs) and possibly in a large number of uncharacterized apoplastic EXT-related proteins (e.g. PERK, Formins, AGP-EXTs hybrids) (Borassi et al. 2016). 59 encoded EXTs in *Arabidopsis thaliana* contain a Tyr-crosslinking motif close to an *O*-glycosylated Ser-$(Hyp)_{3-5}$ (Showalter et al., 2010; Marzol et al. 2018). EXT Tyr-mediated crosslinking is catalyzed by apoplastic peroxidases (Schnabelrauch et al., 1996; Jackson et al., 2001) and allows them to form glycoprotein networks in the cell wall, which influences de novo plant cell wall

119 formation during embryo development (Cannon et al., 2008) and in polar cell expansion
120 processes (Velasquez et al. 2011; 2015). Since CEPs can cleave *O*-glycosylated EXTs (Hierl et
121 al., 2014), thus acting as cell wall-weakening agents, this lends credence to the idea that CEPs
122 may play a pivotal role in cell elongation. Prior to this study, we determined that at least six
123 EXTs (EXT6–7, 12–14, 18) co-regulated at the transcriptional level play a crucial role in the
124 polar-cell expansion process, specifically in RHs (Velasquez et al. 2011; Velasquez et al 2015;
125 Marzol et al. 2018) In this process, Leucine Rich Extensins 1 and 2 (LRX1 and LRX2) were also
126 found to be essential (Baumberger 2001, 2003; Ringli 2010). Pollen EXTs (PEXs) and LRXs were
127 also recently linked to polar growth regulation in pollen tubes (Sede et al. 2018; Ndinyanka
128 Fabrice et al., 2017; Wang et al., 2018), highlighting a conserved role of these EXT and EXT-
129 related proteins in polar growth.

130 On the basis of these previous findings, we hypothesized that Arabidopsis AtCEPs may play a
131 role in polar-growth regulation linked to the processing of *O*-glycosylated EXT and EXT-related
132 proteins processing and possibly other substrates during their maturation along the secretory
133 pathway. Here, we provide evidence that, indeed, AtCEPs negatively regulate levels of EXT
134 secretion/insolubilization at the cell-wall of root hairs (RHs) and retrain their growth.

135

136 **Results and Discussion**

137 Expression of Arabidopsis AtCEPs has been previously analysed using functional reporter
138 constructs that include the coding sequences of AtCEP1 and AtCEP2 under the control of their
139 respective regulatory regions of 2.0 Kb fragment upstream of the start codon, with HA and
140 fluorescent protein tags, either GFP or mCherry (AtCEP1pro:PRE-PRO-3xHA-EGFP-AtCEP1-
141 KDEL and AtCEP2pro:PRE-PRO-3xHA-mCherry-AtCEP2-KDEL) inserted between the pro-
142 peptide and the mature enzyme sequence (Howing et al. 2014 and Hierl et al. 2014).
143 Intriguingly, it was reported that AtCEP2pro:PRE-PRO-3xHA-mCherry-AtCEP2-KDEL is
144 expressed specifically in non-protruding cell files of the hypocotyl, the cell files where stomata
145 are formed, but not in protruding cell files (Hierl et al., 2014). Interestingly, the alternating
146 pattern of non-protruding and protruding cell files in the hypocotyl is controlled by common
147 mechanisms to the alternating pattern of root-hair cell (root trichoblast) and non-root-hair
148 cell (root atrichoblast) files in the root. Hypocotyl non-protruding cells and root trichoblasts
149 are always positioned over an anticlinal cell wall of the underlying cortex and lack expression
150 of cell fate regulators of GL2 and WER and the enhancer-trap marker J2301, whereas
151 hypocotyl protruding cells and root atrichoblast are positioned over a periclinal cortex cell
152 wall and express the J2301 marker and GL2 and WER, which block development of stomata or
153 RHs in these cell files (Berger et al.,1998, Grierson et al., 2014). Importantly, we found that
154 AtCEP2pro:PRE-PRO-3xHA-mCherry-AtCEP2-KDEL is expressed in root epidermis exclusively in
155 the trichoblasts (**Figure 1A-B; Figure S1-S2**), further supporting that root-hair cell files share
156 specification mechanisms and characteristics with non-protruding cell files of the hypocotyl

157 (Berger et al.,1998, Grierson et al., 2014). AtCEP1pro:PRE-PRO-3xHA-EGFP-AtCEP1-KDEL was
158 also specifically expressed in root trichoblasts (**Figure 1A-B; Figure S1**). In these cells, the
159 mCherry-AtCEP2 fusion protein was found in mobile punctate structures, consistent with it
160 being localized in the endomembrane system. To determine the nature of those organelles,
161 we analysed for co-localization with established markers for different compartments (**Figure**
162 **2A**). The AtCEP2 labelled puncta did not co-localize with markers for the Golgi apparatus
163 NAG1-GFP (0.06+-0.13) and N-ST-YFP (0.29+-0.16) (**Figure 2A**). However, we found higher co-
164 localization levels in round or spindled shaped compartments with the ER lumenal marker SP-
165 GFP-KDEL (0.63+-0.16), indicating that AtCEP2 might reside in an ER-derived compartment in
166 root trichoblasts (**Figure 2B**). Indeed, AtCEP2 was observed in ER-derived compartments that
167 resembled ricinosomes and ER-Bodies in leaf, hypocotyl, and root cap cells (Hierl et al. 2014;
168 Howing et al. 2014). In addition, CEP2 mCherry was not detected in the apoplast space when
169 plasmolysis was performed in the root hairs (**Figure 2C**). On the other hand, apoplast
170 targeting of AtCEPs has not been reported previously, possibly indicating that AtCEPs process
171 their substrates within the secretory pathway. This confirms that AtCEP2 is primarily targeted
172 to the ER compartment in root trichoblasts. We cannot rule out the possibility of a low level
173 of an apoplast AtCEP2 expression. To analyse the expression of *AtCEP3*, we used a promoter
174 fragment of 2-0Kb to drive GFP expression. *AtCEP3pro::GFP* fluorescence was also high in root
175 trichoblasts, although not specific to this root epidermal cell-type (**Figure 1A-B; Figure S1-S2**).
176 However, the specific expression of AtCEP1 and AtCEP2 in root trichoblast cells and the high
177 expression of AtCEP3 indicates that these genes may play a role in growth of these specialized
178 cells. To address if they are involved in RH polar growth we isolated *cep* T-DNA mutants
179 (**Table S2** and **Figure 1C**). We characterized at least two T-DNA alleles for each *AtCEP* gene.
180 Single mutants for *AtCEP1*, *AtCEP2* and *AtCEP3* showed similar phenotype to Wt Col-0 (**Figure**
181 **S3**) while the double mutants *atcep1-3 atcep3-2* and *atcep1-3 atcep2-2* showed increased RH
182 growth (up to 20% longer) when compared to Wt Col-0 (**Figure 1D**). These suggested that all
183 three AtCEPs, AtCEP1-AtCEP3, redundantly restrict RH growth. We reasoned then that
184 increased levels of these proteins should shorten RH length. Together, these results indicate
185 that Arabidopsis AtCEP1-AtCEP3 proteins are expressed in RHs where they negatively regulate
186 RH cell growth.

187 NAC1 was previously identified as a regulator of lateral root development and *de novo* root
188 organogenesis (Xie et al., 2000; Chen et al., 2016). Since NAC1 was shown to control *AtCEP1*
189 and *AtCEP2* expression during *de novo* root organogenesis (Chen et al. 2016), we tested if a
190 similar regulation could be taking place in RHs. Indeed, *in silico* analysis (eFP browser and
191 Root Cell Atlas) and characterization of a *NAC1pro:GFP* reporter line supports that *NAC1* is
192 highly expressed in root trichoblasts, specifically in the later stages of their development
193 (**Figure 3A-B**; **Figure S4**). Moreover, a *nac1-2* null mutant displays significantly longer RHs than
194 Wt plants (**Figure 3B**). In addition, when we expressed *NAC1* fused to the repression domain
195 SRDX (Hiratsu et al., 2003) to specifically suppress the expression of NAC1 target gene
196 (35Spro::NAC1-SRDX1-1 and 35Spro::NAC1-SRDX1-2 lines) we observed an elongated RH

197 phenotype (**Figure 3B**). Then, to analyse if *NAC1* overexpression would trigger a direct effects
198 on RH growth possibly by upregulation of AtCEP1/AtCEP2, we used the pER8:3pro::×FLAG-
199 NAC1 β-estradiol-inducible line (Zuo et al., 2000). In the presence of estradiol, an 75-fold
200 induction of *NAC1* levels was observed (**Figure S5**). We then tested if the transcription factor
201 NAC1 activates *AtCEP1-AtCEP3* expression in developing roots, as was shown for *de novo*
202 adventitious root formation assay (Chen et al. 2016). The estradiol-inducible NAC1-FLAG line
203 increased *CEP1* expression by 1.6 folds and *CEP2* by 4-folds while no changes were detected
204 for *CEP3*. (**Figure S5**). The *nac1-2* mutant showed significantly lower levels of transcripts of all
205 three AtCEPs, AtCEP1-AtCEP3 (**Figure 3C**). Together, these results indicate that NAC1 activates
206 the expression of *AtCEP1-AtCEP3*, and in consequence, controls RH growth, possibly through
207 their EXT-processing activity. To determine if NAC1 controls the expression of *AtCEP* genes by
208 direct binding to their promoter regions, we searched for putative NAC-binding sites in open
209 chromatin regions, according to publicly available ATAC-Seq datasets (Maher et al., 2018).
210 According to ChIP-qPCR using pER8:3pro::×FLAG-NAC1 plants (60x induction) and anti-FLAG
211 antibodies, *AtCEP2* and *AtCEP3* appeared as direct targets (**Figure 3D**), as revealed in
212 comparison to the previously identified direct target *E2Fa* (Xie et al. 2023).

213 In previous studies, AtCEPs were shown to be involved in the processing of EXT proteins
214 (Greenwood et al., 2005; Helm et al., 2008; Hierl et al., 2012). We thus tested if the reduction
215 of AtCEP activity in the mutants had an effect on the EXTs secreted and insolubilized in the RH
216 cell walls. To this end, we used an EXT-reporter carrying a tdTomato tag (SS-TOM-Long-EXT)
217 that is resistant to the acidic pH, characteristic of cell wall apoplast (**Figure 4A**). Importantly,
218 expression of the reporter did not affected the polar growth of RHs (Martinez Pacheco et al.
219 2022), making it an ideal probe for monitoring *in situ* alterations in the arrangement of cell
220 wall EXTs. We measured the cell wall fluorescence signal from the SS-TOM-Long-EXT
221 construct in the apical zones of RHs under plasmolysis. Plasmolysis allowed us to retract the
222 plasma membrane and detect the EXT-signal coming specifically from the cell walls.
223 Interestingly, cell wall stabilization/insolubility of SS-TOM-Long-EXT in the RH tip was
224 drastically reduced in *cep1 cep3* double mutant when compared to Wt Col-0 plants. Thus, the
225 SS-TOM-Long-EXT reporter tested in the apical zone of the RHs is modified by deficient AtCEPs
226 activities possibly during the EXT processing in the secretory pathway. Since EXTs
227 insolubilization in the cell walls of growing RHs is regulated by several factors including the
228 Reactive Oxygen Species (ROS) homeostasis (Martinez Pacheco et al. 2022; Marzol et al.
229 2022), we tested if the effect of these AtCEPs might affect global ROS levels. We measured
230 total cytoplasmic ROS ($_{cyt}H_2O_2$) with the hydrogen peroxide-selective dye Peroxy-Orange 1
231 (PO1), as a permeable boronate-based dye that is non-fluorescent in its reduced form, but
232 becomes fluorescent when irreversibly oxidized by H_2O_2 (Dickinson et al., 2010). Apoplastic
233 ROS ($_{apo}H_2O_2$) levels were determined in the RH tips with the cell-impermeable Amplex™
234 UltraRed Reagent (Mangano et al. 2016; Matinez-Pacheco et al. 2022; Marzol et al. 2022)
235 (**Figure 4B**). The *atcep1-3 atcep3-2* showed higher levels of $_{apo}H_2O_2$ in RH tips compared to
236 Col-0, whereas the $_{cyt}H_2O_2$ were similar in both genotypes. This indicates that ROS

237 homeostasis is also changed in the mutant background, which can also affect the EXTs
238 insolubilization in the cell walls.

239 Finally, to test if AtCEP1-AtCEP3 might be able to interact with single-chain EXTs, we
240 performed homology modeling with one cysteine endopeptidase of RcCysEP and a cysteine
241 protease from *Ambrosia artemisiifolia* (pdbs 1S4V and 5EF4 respectively) known to be able to
242 cleave and process EXT-like substrates under *in vitro* conditions. AtCEP1-AtCEP3 proteins
243 share a sequence identity of 66-74% with the most well-characterized *Ricinus communis*
244 RcCysEP (**Figure S6**). By *docking* analysis, we obtained interaction energies (Kcal/mol) for all
245 three AtCEPs and they were compared to RcCysEP 1SV4. We analyzed docking with four
246 different short EXT peptides from non-hydroxylated to fully *O*-glycosylated peptide (Marzol et
247 al. 2016) (**Figure S7**). It was previously shown that mutants carrying under-*O*-glycosylated
248 EXTs and related EXT-proteins have severe defects in RH growth (Velasquez et al. 2011;
249 Velasquez et al. 2015). Our docking results for these three AtCEPs showed consistent
250 interaction energy differences that depend on the EXT glycosylation state, being higher for
251 non-*O*-glycosylated species. In general, we observed higher interaction energies (higher
252 negative values) for (non)-hydroxylated EXT species than for *O*-glycosylated EXT variants.
253 When we compared interaction energies among different AtCEPs interacting with EXT
254 substrates, we observed that AtCEP1 and AtCEP3 displayed the highest interaction activity
255 with the (non)-hydroxylated EXT species (**Figure S7**). Overall, this likely indicates that AtCEP1
256 and AtCEP3 might interact with EXT substrates and possibly catalyse proteolysis in open
257 regions of the EXT backbones with little or no *O*-glycosylation while CEP2 might prefer *O*-
258 Glycosylated regions. This is in agreement with previous studies suggesting that high levels of
259 *O*-glycosylation in certain proteins physically restrict its degradation.

260

261 **Conclusions**

262 It was previously considered that up-regulation of AtCEPs was related to the processing of EXT
263 since EXT promotes wound healing, and this might be a barrier for the emergence of
264 regenerated root tips. Therefore, it was hypothesized that the NAC1-AtCEPs pathway
265 antagonizes EXT-mediated wound healing, and this allows the emergence of regenerated root
266 tips (Chen et al. 2016). However the overall results in our study suggest that NAC1 directly
267 activates AtCEP1 and AtCEP2 expression, which in turn represses polar-cell expansion in
268 growing RHs. By a colocalization analysis with several subcellular markers, we detected
269 AtCEP2 in ER-derived compartments but not in the apoplast. Based on our results, it is
270 plausible that AtCEP1-AtCEP3 could act together as components on the EXT and EXT-related
271 protein quality control program and proper EXTs protein processing. So far there is no
272 information regarding the existence of a quality control pathway for *O*-glycosylated proteins
273 in the same manner to the well-known and conserved CNX (calnexin)/calreticulin lectins
274 linked to ERAD (ER-associated degradation)-program (e.g. with OS9, HRD3/SEL1L components)

275 as it happens for misfolded *N*-glycosylated proteins (Su et al. 2011; Su et al. 2012; Strasser
276 2016). It is also unknown how the *O*-glycosylation machinery required for a proper processing
277 of EXTs and EXT-related proteins in the secretory pathway (Velásquez et al. 2012; Marzol et al.
278 2018) are coordinated and controlled. Our findings pave the way for the discovery of novel
279 functions for AtCEPs in cells that are not undergoing PCD but are characterized by extensive
280 cell wall expansion or remodelling, possibly as a result of EXTs cleavage. The involvement of a
281 protease in cell wall remodelling indicates the significance of the protein component of the
282 cell wall in this process. Insights into the underlying mechanisms, such as the membrane
283 fusion of ricinosomes with the plasma membrane during root development, similar to other
284 ER-derived vesicles, will be intriguing hypothesis to investigate. Recently, a vacuolar
285 processing enzyme (βVPE) was found to control the maturation of AtCEP1 transforming this
286 pro-protease into mature protease while in *vpe* mutants, the maturation of AtCEP1 and other
287 proteases was severely inhibited (Cheng et al. 2020). It is still unclear if VPE may be also acting
288 in root trichoblasts to control AtCEPs processing. Root trichoblasts provide an excellent model
289 system to dissect the molecular components of the NAC1-AtCEPs-EXT *O*-glycosylation
290 pathway required for polar-growth.

291

292 **Experimental Procedures**

293 **Plant and Growth Conditions***. Arabidopsis thaliana* Columbia-0 (Col-0) was used as the Wt
294 genotype in all experiments. All mutants and transgenic lines tested are in this ecotype.
295 Seedlings were germinated on agar plates in a Percival incubator at 22°C in a growth room
296 with 16h light/8h dark cycles for 7-10 days at 140 µmol $m^{-2}s^{-1}$ light intensity. Plants were
297 transferred to soil for growth under the same conditions as previously described at 22°C. For
298 identification of T-DNA knockout lines, genomic DNA was extracted from rosette leaves.
299 Confirmation by PCR of a single and multiple T-DNA insertions in the target AtCEP and NAC
300 genes were performed using an insertion-specific LBb1 or LBb1.3 (for SALK lines) or Lb3 (for
301 SAIL lines) primer in addition to one gene-specific primer. To ensure gene disruptions, PCR
302 was also run using two gene-specific primers, expecting bands corresponding to fragments
303 larger than in Wt. In this way, we isolated homozygous lines (for all the genes mentioned
304 above). Mutant list is detailed in **Table S1**. Lines expressing AtCEP2pro:pre-pro-3xHA-
305 mCherry-AtCEP2-KDEL were crossed with ER and Golgi marker lines to obtain the double
306 transgenic AtCEP2 + organelle marker

307 **Root Hair Phenotype.** Seeds were surface sterilized and stratified in darkness for 3 d at 4°C
308 and they were grown *in vitro* on a specific condition and medium in a plant growth chamber
309 in continuous light (120 mol s-1 m-2) at 22°C. The quantitative analyses of RH phenotypes of
310 Col-0 and transgenic lines were made the last day of the growth conditions described in the
311 two previous sections. Images were captured using an Olympus SZX7 Zoom Stereo
312 Microscope (Olympus, Tokyo, Japan) equipped with a Q-Colors digital camera and Q CAPTURE

313 PRO 7 software (Olympus). Results were expressed as the mean SD using the GRAPHPAD
314 PRISM 8.0.1 (GraphPad Software, Boston, MA, USA) statistical analysis software. Results are
315 representative of three independent experiments, each involving 15–20 roots.

316 **AtCEP imaging.** Root hairs were ratio imaged with the Zeiss LSM 510 laser scanning confocal
317 microscope (Carl Zeiss) using a 40X oil-immersion, 1.2 numerical aperture objective. EGFP
318 (473–505nm) and mCherry (526–536 nm) emissions were collected using a 458-nm primary
319 dichroic mirror and the Meta-detector of the microscope. Bright-field images were acquired
320 simultaneously using the transmission detector of the microscope. For time-lapse analysis,
321 images were collected every 3 or 5 s. Image sequences were analyzed using the Template
322 Matching and Slice Alignment plug-in for ImageJ. Fluorescence intensity was measured in 7
323 µm ROI at the RH apex.

324 **Transcriptional reporter generation.** Vectors based on the Gateway cloning technology
325 (Invitrogen) were used for all manipulations. Promoter regions (2Kb) were PCR-amplified with
326 AttB recombination sites. PCR products were first recombined in pDONOR207 and transferred
327 into pMDC111. Transgenic lines used in this study are described in **Table S2**.

328 **AtCEPs expression.** To quantify AtCEP1 and AtCEP2 expression levels, lines AtCEP1pro:3xHA-
329 EGFP-KDEL AtCEP2pro: 3xHA-mCherry-KDEL were used. The fluorescence intensity of GFP and
330 mCherry was measured respectively. All RHs growth stages were measured. Ten days old
331 seedlings were removed from the medium and placed in a slide containing a drop of liquid MS
332 0.5X in the dark, and images were obtained using a Zeiss Imager A2 epifluorescence
333 microscope. The objective used was 10X, 0.3 numerical aperture, exposure time 2 seconds.
334 The lasers used were suitable for each fluorophore: GFP (GFP λ max ex. = 488 nm, λ max em. =
335 507 nm) and mCherry (λ max ex. = 536 nm, λ max em. = 632 nm) The Wt Col-0 line was used
336 to rule out autofluorescence noise. The images were analyzed using ImageJ 1.50b software.
337 To measure fluorescence intensity levels (represented in arbitrary units: UA), both a circular
338 region of interest within the RH apex (ROI) and the total area of RH were selected. All RHs
339 from 6 seedlings were analyzed. The reported values are the mean ± standard error (mean ±
340 SEM).

341 **Subcellular localization of AtCEP2.** Lines expressing CEP2pro:pre-pro-3xHA-mCherry-CEP2-
342 KDEL were crossed with ER and Golgi marker lines to obtain the double transgenic CEP2 +
343 organelle marker. Co-localization analysis was performed using the BIOP implementation
344 (Battistella et al. 2019) of the JACoP-plugin (Bolte and Cordelières 2006) in ImageJ (1.53t) on
345 individual root hairs for which ROIs (Region Of Interest) were drawn manually. Background
346 intensity was subtracted from each channel as the mean intensity of the autofluorescence
347 control + 2SD. Different marker expression levels excluded the usage of fixed cutoff values for
348 all images, so the histogram-derived Otsu method was chosen based on visual inspection of
349 the thresholded images for both channels. To compare the relative localization of
350 CEP2pro:pre-pro-3xHA-mCherry-CEP2-KDEL (Ch2) in each of the different subcellular

351 compartments (Ch1), we used Mander's M2 overlap coefficient (Manders et al. 1993) to
352 measure the proportion of positive pixels in Ch2 that co-occur with positive pixels in Ch1.
353 Confocal microscopy images were acquired on a Zeiss LSM710 microscope with an EC Plan-
354 Neofluar 40x/1.30 oil objective. Images were acquired sequentially on different tracks in
355 order to avoid excitation and emission bleed-through using the following emission ranges for
356 the individual channels (8-bit pixel depth): Ch1 519–589 nm, Ch2 594-690 nm. Pixel size was
357 set at 100 nm following Nyquist sampling criterion and pinhole was adjusted to obtain a 3.6
358 µm thick optical slice. For each experimental replicate, 15-25 total individual root hairs from
359 five different plants per subcellular compartment marker were imaged.

360 **Chromatin immunoprecipitation Assay.** Chromatin immunoprecipitation (ChIP) assays were
361 performed on pER8:3xFLAG-NAC1 plants (Chen et.al 2016, DOI: 10.1104/pp.15.01733) mainly
362 as described in Ariel et al. (2020). Plants were grown for 10 days in plates containing MS 0,5X
363 medium (pH 5,7; 0.8% agar) placed vertically in a culture chamber at 22°C and continuous
364 light (140µmol/m2.sec). After 10 days, the plates were placed horizontally and treated with β-
365 estradiol 10 µM solution for 3h. The expression of NAC1 was checked by qPCR
366 (supplementary table Sx). Chromatin was cross-linked with formaldehyde 1% for 10 min at
367 room temperature. Cross-linking was stopped by adding glycine (125 mM final concentration)
368 and incubating for 10 min at room temperature. Crosslinked chromatin was extracted by cell
369 resuspension, centrifugation, cell membrane lysis, and sucrose gradient as previously
370 described (Ariel et al., 2020). Nuclei were resuspended in Nuclei Lysis Buffer and chromatin
371 was sonicated using a water bath Bioruptor Pico (Diagenode; 30s on / 30s off pulses, at high
372 intensity for 10 cycles). Chromatin samples were incubated for 12h at 4°C with Protein G
373 Dynabeads (Invitrogen) precoated with the antibodies anti-FLAG (Abcam ab18230) or anti-IgG
374 (Abcam ab6702) as a negative control. Immunoprecipitated DNA was recovered using
375 Phenol:Chloroform:Isoamilic Acid (25:24:1; Sigma) and analyzed by qPCR using the primers
376 listed in Supplementary Table Sx. A region upstream E2Fa gene was used as a positive control
377 (Xie et al. 2023). ACTIN was used as a negative control. Untreated sonicated chromatin was
378 processed in parallel and considered the input sample. The GraphPad Prism 6 software was
379 used to analyze the data and produce the graphs.

380 **Apoplastic and cytoplasmic ROS measurements**. To measure ROS levels in root trichoblasts, 8
381 days-old Arabidopsis seedlings grown in continuous light were used. For cytoplasmic ROS, the
382 seedlings were incubated in darkness for 10 min with H2O2 and were visualized with Peroxy-
383 Orange 1 (PO1). PO1 was dissolved in DMSO to make a 500 µM stock and was further diluted
384 in water to make a 50 µM working solution. Seedlings were incubated in PO1 for 15 min in the
385 dark and were then rinsed with water and mounted in water for imaging and observed with
386 Zeiss Imager A2 Epifluorescence Microscope (Zeiss, Germany) (Plain Apochromat 40X/1.2 WI
387 objective, exposure time 25 ms). Images were analyzed using ImageJ software. To measure
388 ROS levels, a circular region of interest was chosen in the zone of the RH tip cytoplasm. To
389 measure apoplastic ROS, the seedlings were incubated with 50 µM Amplex™ UltraRed
390 Reagent (AUR) (Molecular Probes, Invitrogen) for 15 min in darkness and rinsed with liquid

391 0.5X MS media (Duchefa, Netherlands). Root hairs were imaged with a Zeiss LSM5 Pascal
392 (Zeiss, Germany)) laser scanning confocal microscope (Excitation 543 nm argon laser;
393 Emission: 560–610 nm, Plain Apochromat 40X/1.2 WI objective). Quantification of the AUR
394 probing fluorescence signal was restricted to apoplastic spaces at the RH tip and quantified
395 using the ImageJ software. Fluorescence AU were expressed as the mean ± SD using the
396 GraphPad Prism 8.0.1 (USA) statistical analysis software. Results of both ROS measurements
397 are representative of two independent experiments, each involving 10–15 roots and
398 approximately, between 10 and 20 RHs per root were observed.

399 **Treatments with *β* -Estradiol.** *β*- Estradiol (Sigma-Aldrich,) was added to 0.5X MS media at a
400 final concentration of 10 µM. The lines ER8pro:AtCEP2 and ER8pro:3×FLAG-NAC1 were grown
401 at 22°C for 4 days + 3 days of *β*- Estradiol induction. Root hairs phenotype was then
402 quantified.

403 **Quantitative reverse transcriptase PCR (qRT-PCR).** Total RNA was isolated from 10-d-old
404 seedling roots (40 for each line) using the RNeasy Plant Mini Kit (Qiagen, Germany). cDNA was
405 synthesized using TOPscript^{TM} RT DryMIX (dT18, Enzynomics, Korea). qRT-PCR analyses were
406 performed using TOPrealTM qPCR 2x PreMIX (SYBR Green, Enzynomics, Korea) and
407 Chromo4™ Four-Color Real-Time Detector (Bio-Rad, USA). Gene-specific signals were
408 normalized relatively to *PP2A* (At1G69960) signals. Each qRT-PCR reaction was performed in
409 triplicate, and each experiment was repeated three times using independent preparations of
410 RNA. Primers used are as listed in **Table S3**.

411 **Modelling and molecular docking between AtCEP1-AtCEP3 and EXTs.** Modeling and
412 molecular docking: cDNA sequences of AtCEPs were retrieved from TAIR (AtCEP1:
413 AT1G05240, AtCEP2: AT3G50990, AtCEP3: AT4G26010) and NCBI Nucleotide DB. Homology
414 modeling was performed using an AtCEP from *Ricinus communis* and from *Ambrosia*
415 *artemisiifolia* using modeller 9.14 (Sali et al. 1993), using the crystal structures 1S4V and 5EF4
416 as templates, available at the protein data bank. 100 structures were generated for each
417 protein and the best scoring one (according to DOPE score) was picked. The *receptor* for the
418 docking runs was generated by the prepare_receptor4 script from the autodock suite, adding
419 hydrogens and constructing bonds. Peptides based on the sequence
420 PYYSPSPKVYYPPPSSYVYPPPPS were used, replacing proline by hydroxyproline, and/or adding
421 *O*-Hyp glycosylation with up to four arabinoses per hydroxyproline in the fully glycosylated
422 peptide and a galactose on the serine, as it is usual in plant *O*-Hyp (Strasser 2016). Ligand
423 starting structure was generated as the most stable structure by molecular dynamics
424 (Velasquez et al. 2015a). All ligand bonds were set to be able to rotate. Docking was
425 performed in two steps, using Autodock vina (Trott et al. 2010). First, an exploratory search
426 over the whole protein surface (exhaustiveness 4) was done, followed by a more exhaustive
427 one (exhaustiveness 8), reducing the search space to a 75x75x75 box centered over the most
428 frequent binding site found in the former run.

429
430

Acknowledgements

We thank ABRC (Ohio State University) for providing T-DNA lines seed lines and Gietl for providing some of the materials used in this study. J.M.E. is investigator of the National Research Council (CONICET) from Argentina. This work was supported by grants from ANPCyT (PICT 2016-0132 and PICT2019-00015 to J.M.E and PICT2018-00577 to E.M.) and from the Spanish Ministry of Science and Innovation MCIN/AEI/10.13039/501100011033 and FEDER "una manera de hacer Europa" (PID2021-128078NB-I00 to E.R.). In addition, this research is also funded by ANID – Programa Iniciativa Científica Milenio ICN17_022, NCN2021_010 and Fondo Nacional de Desarrollo Científico y Tecnológico [1200010] to J.M.E. The authors gratefully acknowledge the Microscopy and Imaging Facility at the Leloir Institute Foundation (FIL) for their support and assistance in the present work.

Author Contribution

D.R.G performed all the experiments and analyzed the data. E.M performed AtCEP expression and analyzed the data. Y.d.C.R. performed ROS experiments. A.H.R and E.A.M. carried out co-localization studies. A.A.A. and A.D.N. carried out the molecular modeling of AtCEPs-EXTs. L.F and F.A. carried out the ChIP experiment and analyzed the data. J.M. P., M.C., V.B.G., L.E.L and G.D.D. analyzed the data. L.X., E.R and J.J.S.S. provided materials, analyzed the co-localization data and wrote the paper. E.R. wrote the paper. J.M.E. designed research, analyzed the data, supervised the project, and wrote the paper. All authors commented on the results and the manuscript. This manuscript has not been published and is not under consideration for publication elsewhere. All the authors have read the manuscript and have approved this submission.

Competing financial interest

The authors declare no competing financial interests. Correspondence and requests for materials should be addressed to J.M.E. (Email: jestevez@leloir.org.ar).

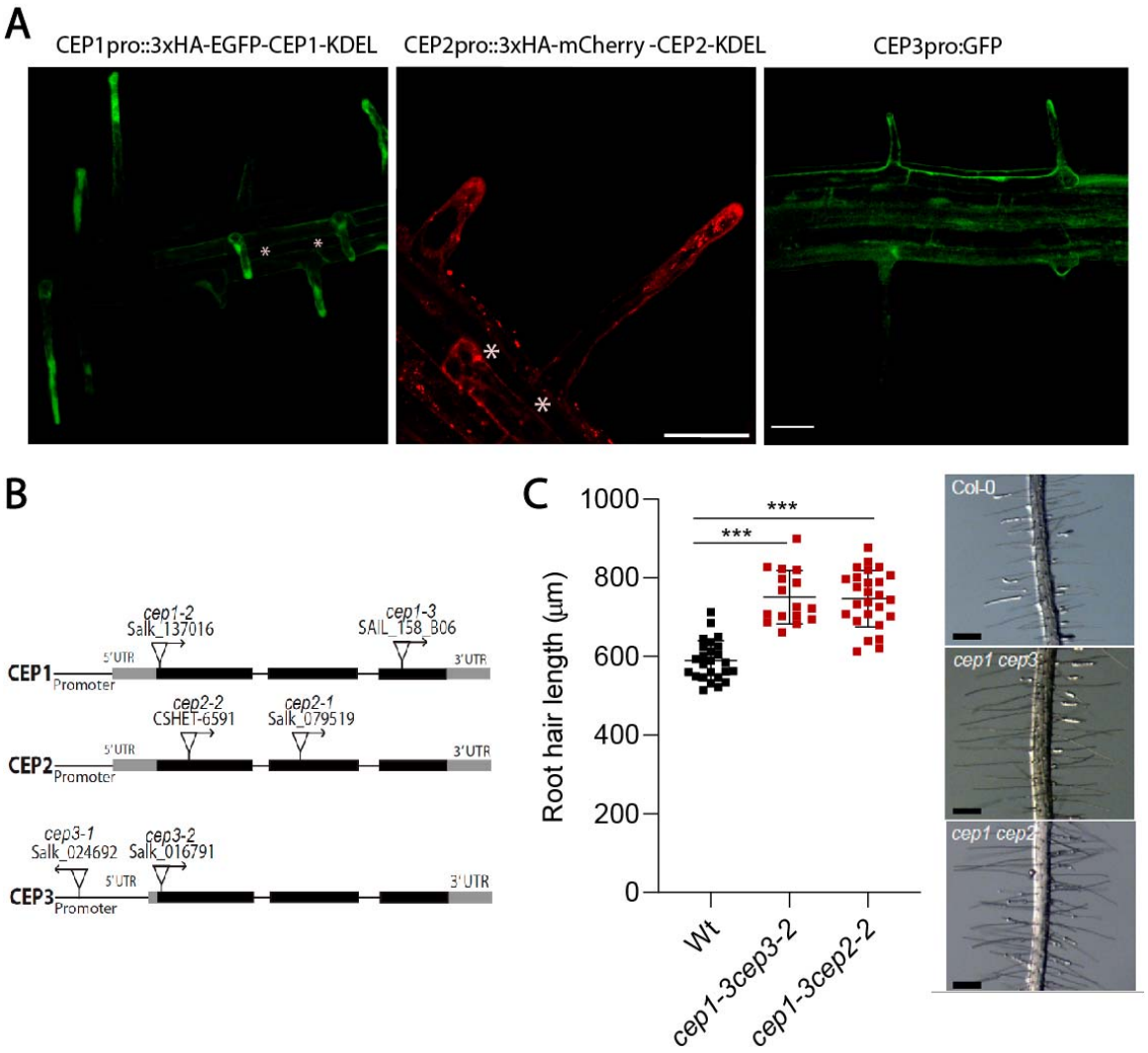

Figure 1. AtCEP1, AtCEP2 and AtCEP3 are expressed in root hairs and negatively regulate root hair growth. (**A**) AtCEP1 and AtCEP2 are expressed in root trichoblasts. Translational reporters for AtCEP1 (AtCEP1pro::PRE-PRO-GFP-KDEL) and AtCEP2 (AtCEP2pro::PRE-PRO-mCherry-AtCEP2-KDEL). AtCEP3 are expressed in both atricoblasts and tricoblasts. Transcriptional reporters of AtCEP3 (AtCEP3proGFP) in the root differentiation zone and specifically in RHs. Scale bar = 200 µm. (*) Indicates lack of expression in atrichoblasts. (**B**) Scheme of AtCEP1, AtCEP2 and AtCEP3 genes showing introns (thin lines), exons (rectangles) and positions of T-DNA insertions. (**C**) Quantitative analysis of RH length (mean ± s.e.m., n= 200) in Wt Col-0 and *ceps* mutants. NS= not significant difference. Data are shown as the mean ± SEM, (n=20). Asterisks indicate significant differences from the Wt according to an ANOVA test with $p<0.05$. (On the right) Selected images of RHs in Wt and in single and double *cep* mutants. Scale bar = 200 µm.

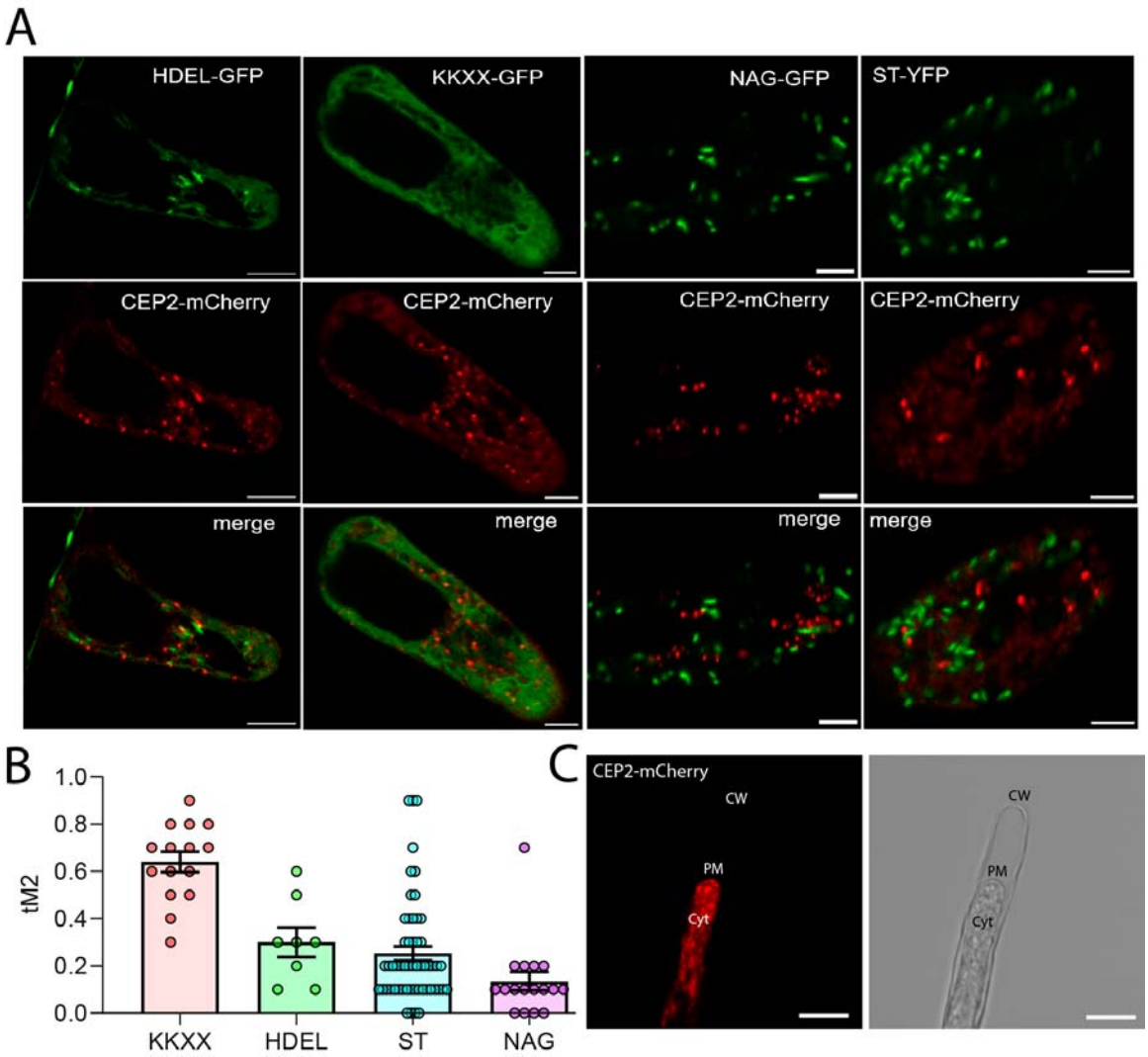

Figure 2. AtCEP2 colocalizes mostly with an ER-membrane marker and, to a lower extent, to Golgi markers in root hair cells. (**A**) Co-localization of AtCEP2-mCherry with markers for different subcellular compartments. Seven-day-old AtCEP2mCherry seedlings were grown (n= 10 roots with 1–5 root hair cells each). HDEL-GFP is a Lumen Endoplasmic reticulum (ER) marker and KKXX-GFP is an ER membrane marker. NAG-GFP is a cis-Golgi marker and ST-YFP is a trans-Golgi network marker. Scale bar 5 µm. (**B**) Quantification of colocalization using Manders correlation coefficient. (**C**) Plasmolyzed root hair to show the lack of signal in the apoplastic regions of AtCEP2-mCherry. Scale bar 20 µm. (CW) Cell Wall; (PM) Plasma membrane; (Cyt) Cytoplasm.

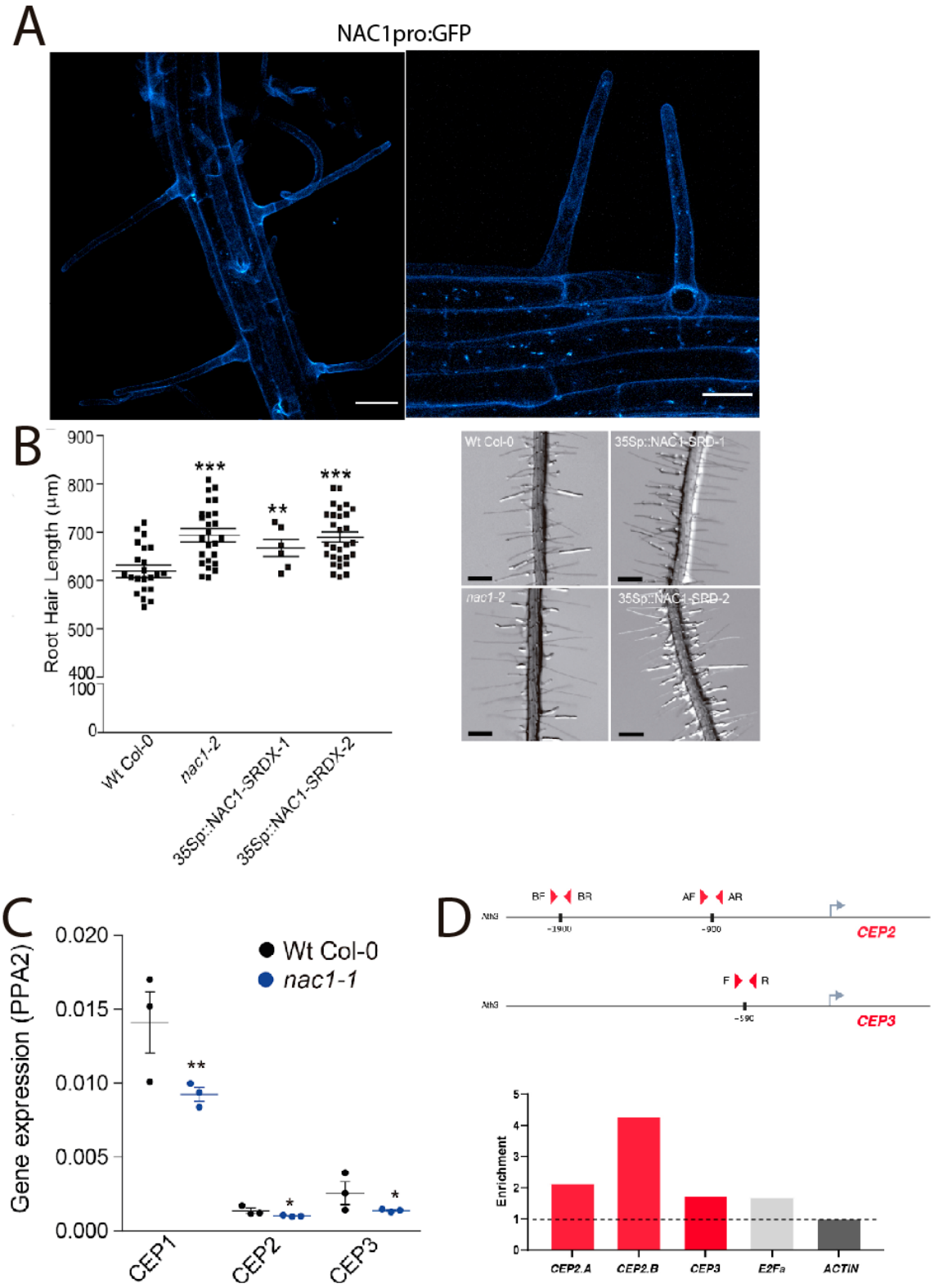

Figure 3. NAC1 is expressed and regulates root hair growth linked to AtCEP1-AtCEP3 expression. (**A**) NAC1pro:GFPexpression in roots and RHs. (**B**) RH phenotype in *nac1-2* mutant and two constitutive negative NAC1 lines. Quantitative analysis of RH length (mean ± s.e.m.,

495 n= 200). Data are shown as the mean ± SEM, (n=20). Asterisks indicate significant differences
496 from the Wt Col-0 according to an ANOVA test with $p<0.05$. (**C**) qPCR analysis of AtCEP1,
497 AtCEP2, and AtCEP3 in Wt Col-0 and *nac1-2* mutants. RNA was extracted from root of
498 seedlings. *PP2A* was used as a control and amplification was performed for 30 cycles. Black
499 arrowheads represent the region amplified by the primers used for the RT-PCR. (**D**) ChIP-qPCR
500 analysis of NAC1 binding to CEP2 and CEP3 promoter regions. Schemes of the loci showing the
501 location of the fragments analyzed by ChIP-qPCR are shown in the upper part. Primers were
502 designed analyzing ATAC-seq experiments in regions where the chromatin is accessible
503 (Maher et al., 2018). The enrichment was measured relative to the negative control ACTIN.
504

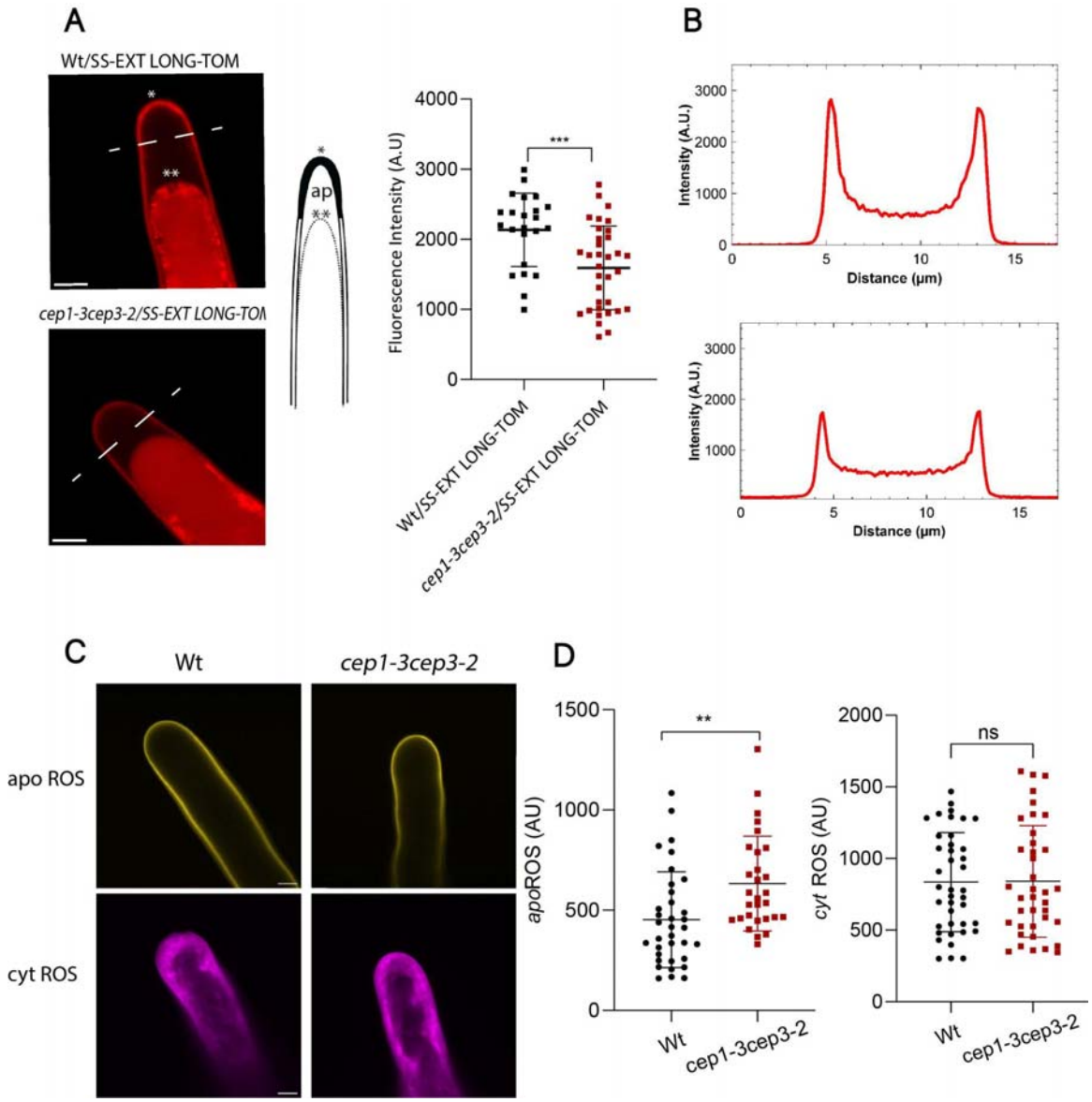

Figure 4. **EXT secretion/insolubilization and apoplastic ROS are affected by AtCEP1-AtCEP3 in root hairs**. (**A**) Signal of SS-EXT LONG-TOM in the apical zone of RHs in the *cep1-3 cep3-2* double mutant. Cells were plasmolyzed with a mannitol 8% solution. In the images: (*) indicates cell surface including the plant cell walls, (**) indicates the retraction of the plasma membrane, (ap) apoplastic space delimited between the plant cell wall and the retracted plasma membrane. Each point in the graph is the signal derived from a single RH tip. Fluorescence AU data are the mean ± SD SD (N = 3), two-way ANOVA followed by a Tukey–Kramer test; (***) p<0.01. Results are representative of two independent experiments. NS = non-significant differences. Scale bars = 5 µm. (**B**) Intensity profiles across a dotted line in the RH tips. (**C**) Cytoplasmic ROS ($_{cyt}$ROS) levels were measured using the hydrogen peroxide-selective dye Peroxy-Orange 1 (PO1) in apical areas of RHs in wild-type (Columbia Col-0) and in the double mutant *cep1-3 cep3-2*. Each point is the signal derived from a single RH tip. Fluorescence AU data are the mean ± SD (N= 20 RHs), two-way ANOVA followed by a Tukey–

519 Kramer test; (**) $p < 0.01$. Results are representative of two independent experiments.
520 Asterisks indicate significant differences. NS = non-significant differences. Scale bars = 2 µm.
521 (**D**) Apoplastic ROS ($_{apo}$ROS) levels were measured with Amplex™ UltraRed in apical areas of
522 RHs in wild-type (Columbia Col-0) and in the double mutant *cep1-3 cep3-2*. Each point in (**D**) is
523 the signal derived from a single RH tip. Fluorescence AU data are the mean ± SD (N =3), two-
524 way ANOVA followed by a Tukey–Kramer test. Results are representative of two independent
525 experiments. Scale bars = 2 µm.

526

527

528

529

530
531

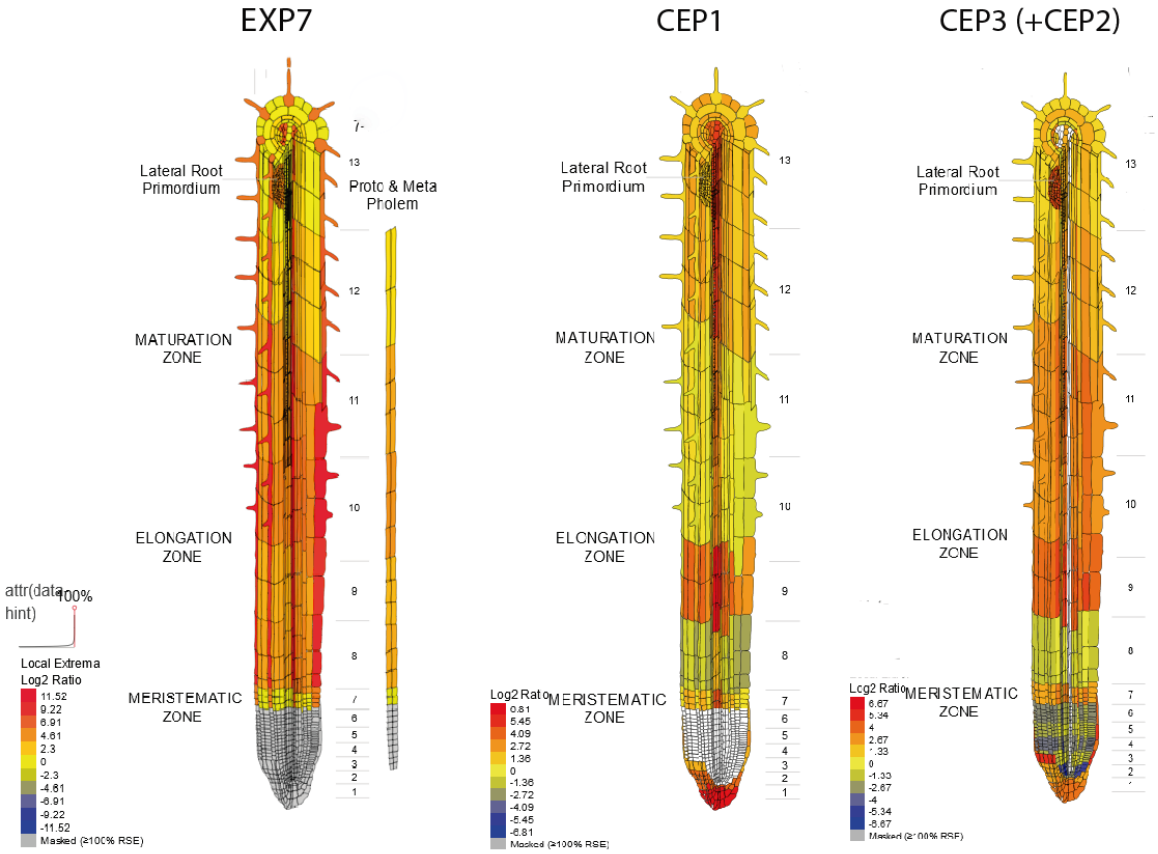

Figure S1. The *in silico* analysis of AtCEPs gene expression using Tissue Specific Root eFP (http://bar.utoronto.ca/eplant/). EXP7 was included as a root hair cell marker.

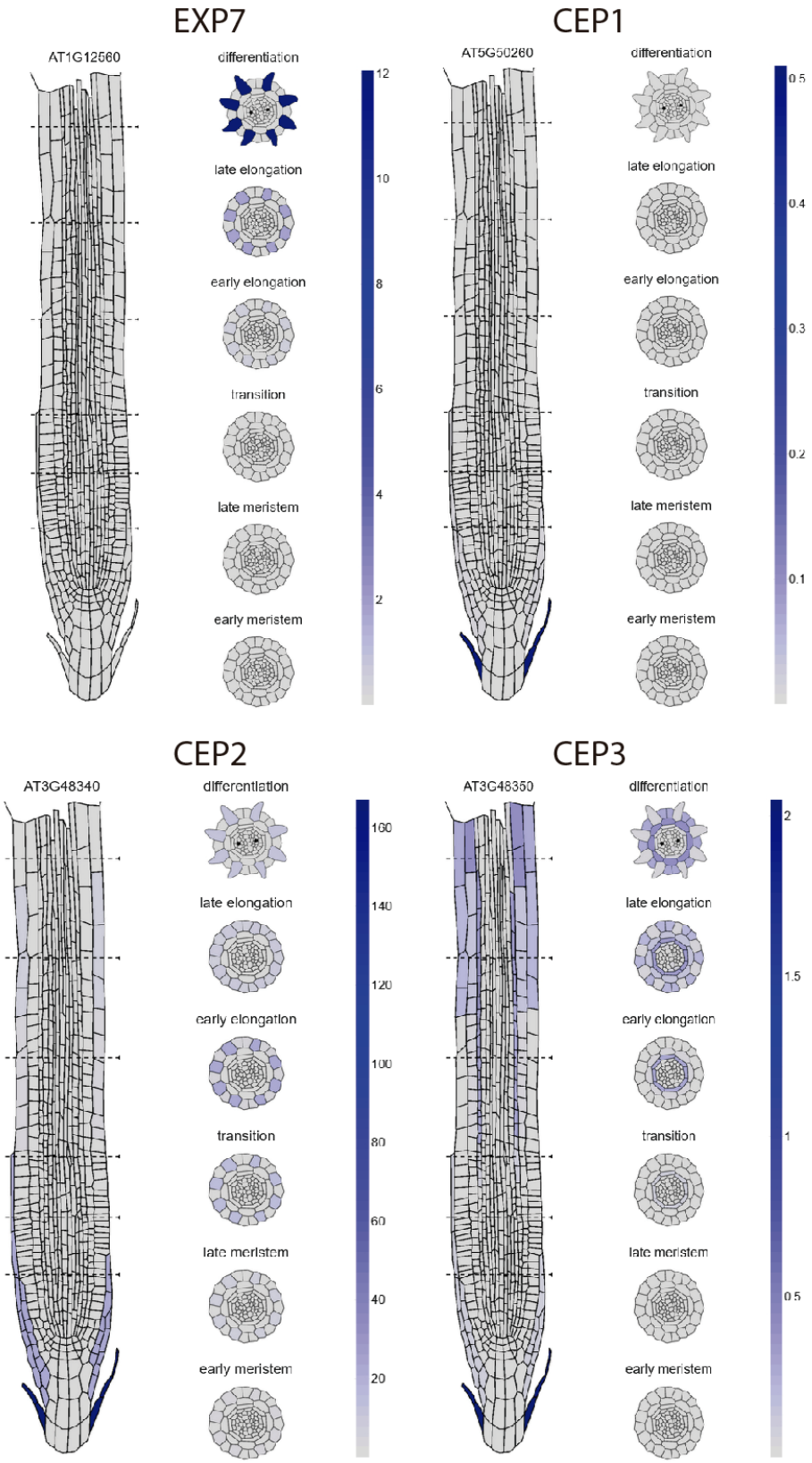

Figure S2. The *in silico* analysis of AtCEP1-AtCEP3 expression using Root Cell Atlas (https://rootcellatlas.org/). EXP7 was included as a root hair cell marker.

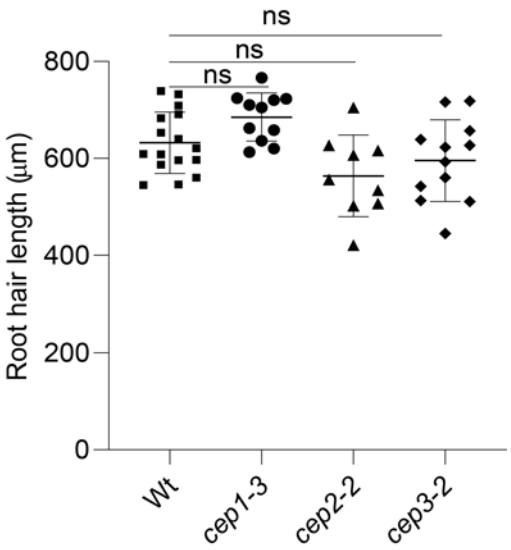

538
539
540 **Figure S3**. **Single *cep* mutants do not perturb root hair growth.** Quantitative analysis of RH
541 length (mean ± s.e.m., n= 200) in Wt Col-0 and in single *cep* mutants. NS= not significant
542 difference. Data are shown as the mean ± SEM, (n=20).
543

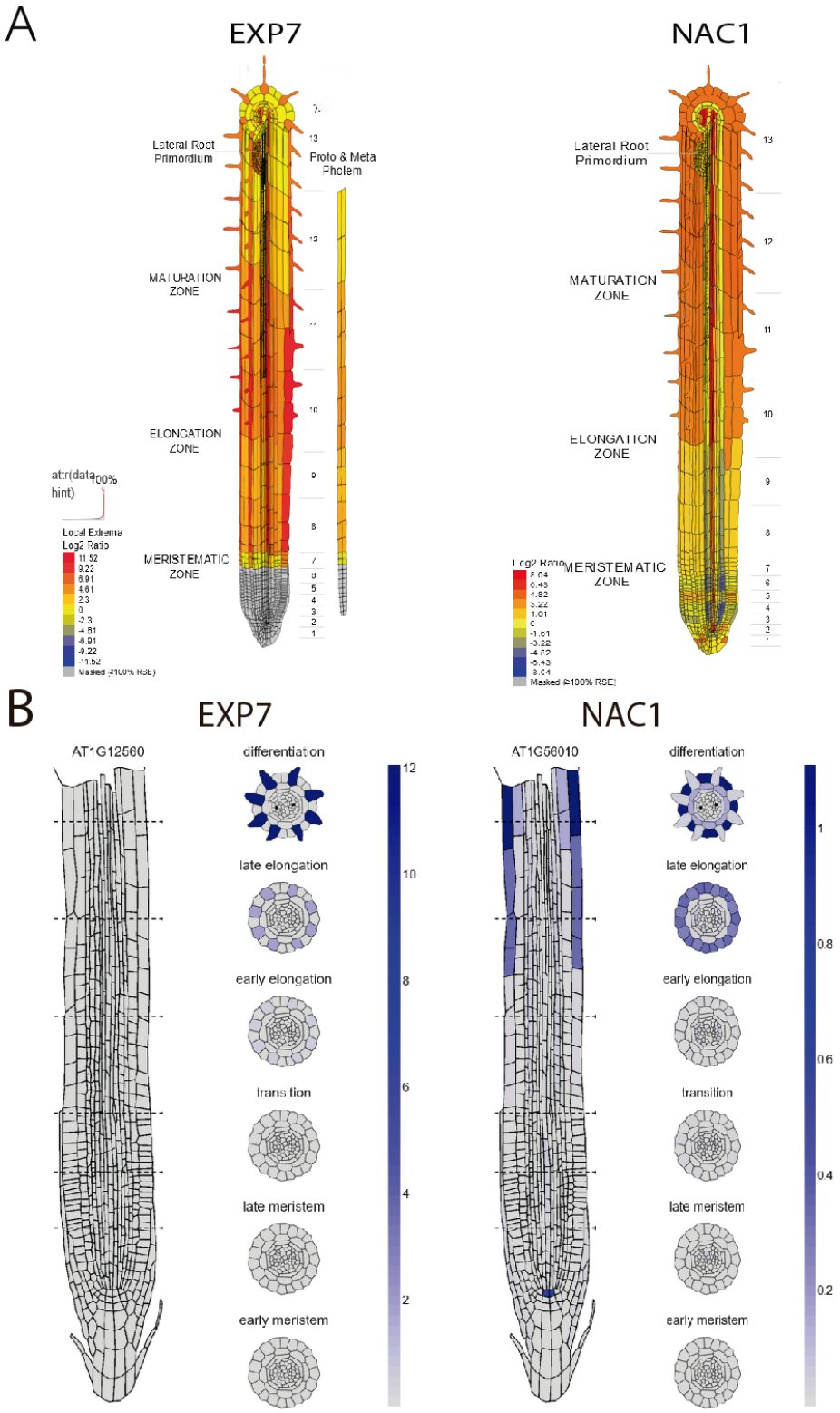

Figure S4. The *in silico* analysis of NAC1 expression using Tissue Specific Root eFP (http://bar.utoronto.ca/eplant/) (**A**) and using Root Cell Atlas (https://rootcellatlas.org/) (**B**). EXP7 was included as a root hair cell marker.

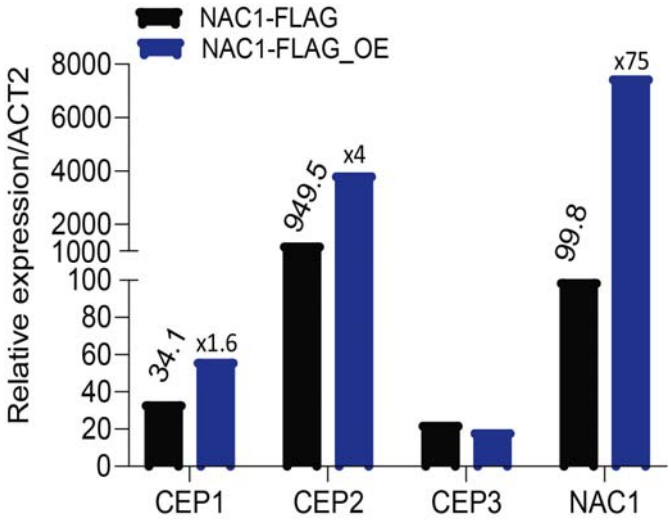

Figure S5. Induction of CEP1 and CEP2 by NAC1-FLAG inducible line (PER8pro:3×FLAG-NAC1). Gene-specific signals were normalized relatively to ACT2.

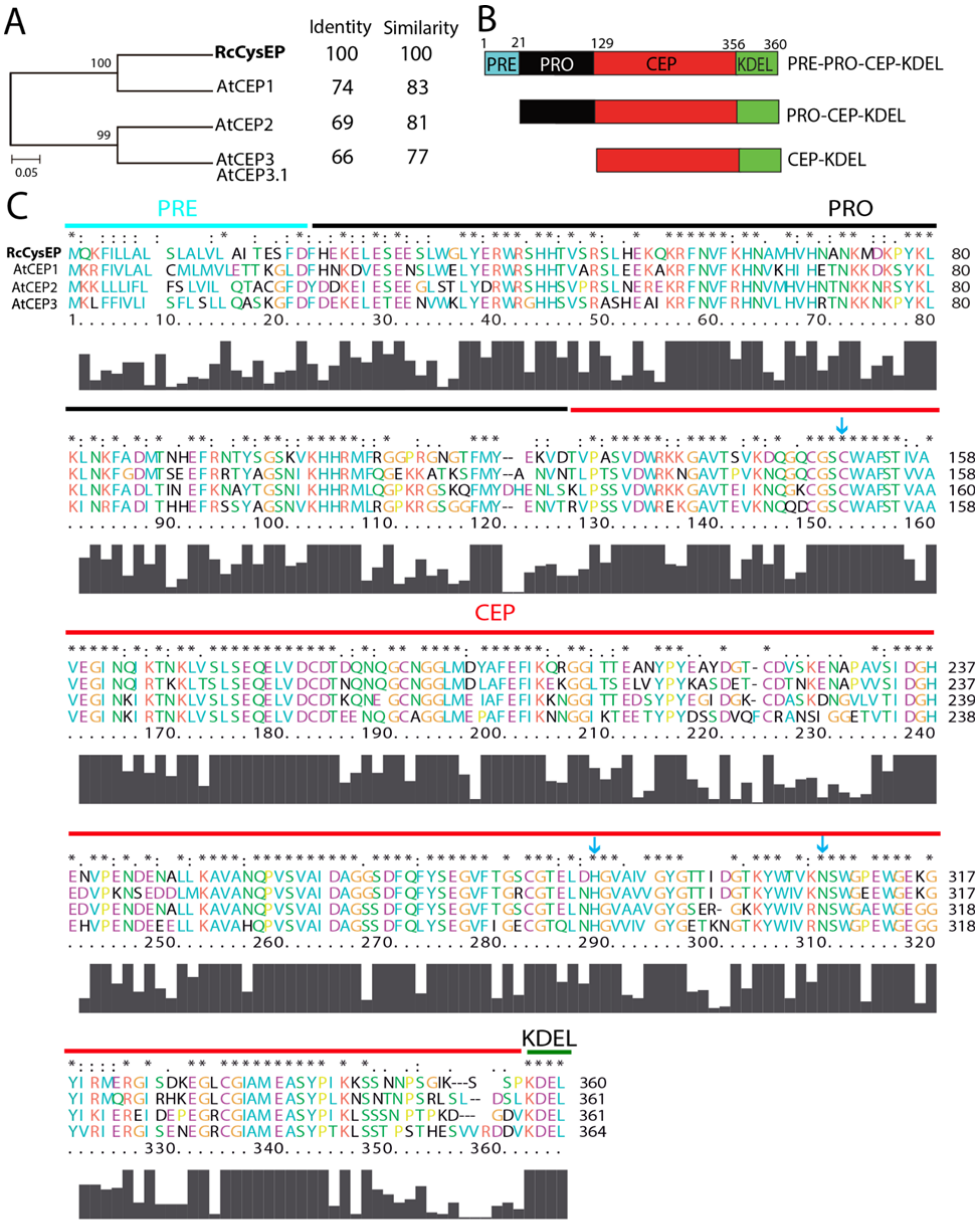

555 CEP3.1ΔKDEL 275YSEVIFGSLSLRQKTSYEKITYQC299

556

557 **Figure S6. Protein alignment and domains of AtCEP1-AtCEP3 sequences from *Arabidopsis***
558 ***thaliana* with Ricinus CEP 1SV4 (RcCysEP).** (**A**) Phylogenetic tree of Arabidopsis AtCEPs and
559 Ricinus AtCEP. The phylogenetic analysis was carried out with MEGA6 (Tamura et al., 2007)
560 using the Maximum Similarity method (Maximum Likelihood) (Saitou and Nei, 1987). The
561 numbers in the nodes indicate the bootstrap values obtained for 1000 iterations. Scale
562 represents the evolutionary distance, expressed as the number of substitutions per amino
563 acid. (**B**) AtCEP protein domains. AtCEPs are synthesized as pre-pro-enzyme, which is then co-
564 translationally synthesized into the ER, where the pre-sequence is removed, and pro-enzyme
565 is finally released from the ricinosomes. KDEL is an ER retention signal peptide. (**C**) AtCEP1-
566 AtCEP3 Protein alignment. PRE, PRO and KDEL domains are indicated.

567

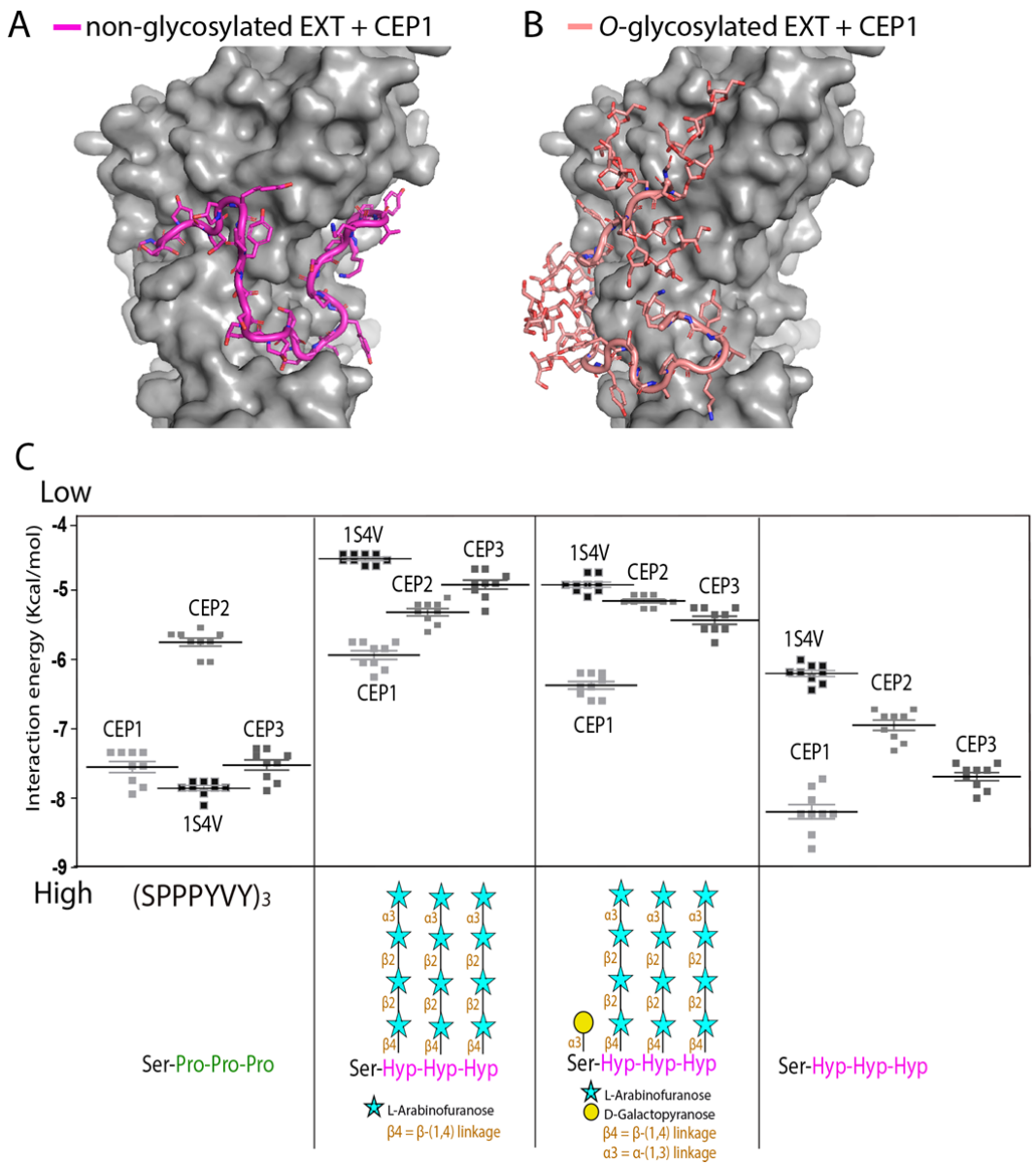

Figure S7. Interaction by an *in silico* docking approach of AtCEP1, AtCEP2 and AtCEP3 with EXT peptides. (**A,B**) Ten docking results for each EXT *O*-glycosylation state are shown superimposed on the AtCEP1 protein surface to evaluate the consistency of docking sites. (**A**) Model of AtCEP1 (protein surface shown in grey) complexed to a non-*O*-glycosylated EXT substrate $(SPPPYVY)_3$ (in magenta). (**B**) Model of AtCEP1 (protein surface shown in gray) complexed to an *O*-glycosylated-EXT substrate (protein and *O*-glycans shown in light red, both depicted as sticks). Arabino-galactosylated EXT peptide = [$(SOOOYVY)_3$-AG]. (**C**) Comparison of the binding energy of different AtCEP1-AtCEP3 and 1S4V (Ricinus AtCEP included as a control) to EXT substrates with different degrees of *O*-glycosylation. (from left to right) A non-hydroxylated EXT peptide $(SPPPYVY)_3$, a hydroxylated but not *O*-glycosylated EXT peptide [$(SOOOYVY)_3$; O=hydroxyproline], only arabinosylated EXT-peptide [$(SOOOYVY)_3$-A], and arabino-galactosylated EXT peptide [$(SOOOYVY)_3$-AG] were analyzed.

582 **Table S1.** Mutant lines used in this study.

NAME	ATG code		Mutant line	Reference
NAC1	*At1g56010*	*nac1-2*	CS1013025	This work
AtCEP1	*At5g50260*	*cep1-2*	SALK_137016	This work
		cep1-3	SAIL_158_B06	(Höwing et al. 2014)
AtCEP2	*At3g48340*	*cep2-1*	SALK_079519	This work
		cep2-2	CSHET_6591	(Hierl et al. 2014)
AtCEP3	*At3g48350*	*cep3-1*	SALK_024692	This work
		cep3-2	SALK_016791	This work

583

584

585 **Table S2.** Transgenic lines used in this study.

NAME	CONSTRUCTION	BACKGROUND	REFERENCE
PER8pro:AtCEP2	promoterPER8::AtCEP2	Wt Col-0	(Chen et al. 2016)
PER8pro:AtCEP1	promoterPER8::AtCEP1	Wt Col-0	(Chen et al. 2016)
PER8pro:3×FLAG-NAC1	promoterPER8::3×FLAG-NAC1	Wt Col-0	(Chen et al. 2016)
NAC1pro:NAC1-GUS	promoterNAC1::NAC1-GUS	Wt Col-0	(Chen et al. 2016)
AtCEP1pro:3xHA-EGFP-AtCEP1-KDEL	promoterAtCEP1:: PRE-PRO-3xHA-EGFP-AtCEP1-KDEL	*cep1-3*	(Höwing et al. 2014)
AtCEP1pro:3xHA-EGFP-KDEL	promoterAtCEP1:: PRE-PRO-3xHA-EGFP-KDEL	*cep1-3*	(Höwing et al. 2014)
AtCEP2pro: 3xHA-mCherry-KDEL	promoterAtCEP2::PRE-PRO-3xHA-mCherry-KDEL	*cep2-2*	(Hierl et al. 2014)
AtCEP2pro:3xHA-mCherry -AtCEP2-KDEL	promoterAtCEP2::PRE-PRO-3xHA-mCherry-AtCEP2KDEL	Wt Col-0	(Hierl et al. 2014)
AtCEP3pro:GFP	promoterAtCEP3::GFP	Wt Col-0	This work
NAC1pro:GFP	promoterNAC1::GFP	Wt Col-0	This work

PP2A RT-F	GTCGACCAAGCGGTTGTGGAGA
PP2A RT-R	ACGCCCAACGAACAAATCACAGA
AtCEP1 RT-F	AAACCAAGGCCAATGCGGGAGTTG
AtCEP1 RT-R	TTCCGCATCTCCCGGTAAACACTC
AtCEP2 RT-F	CCGGTTCCAACATCAAGCATCAC
AtCEP2 RT-R	AGATCCGTAAACACTCCCTCTG
NAC1 RT-F	TGAGCTCTCCAAAGGAAGACTGG
NAC1 RT-R	ACAGAATGAGTCGAGGCCTGTG
CEP2 CHIP A F	ATGGGCTGCGCCAAATGTTC
CEP2 CHIP A R	ACGTCTTAAACCATGCACCGA
CEP2 CHIP B F	TCGGACTTTTTGATTGGAATCCTCT
CEP2 CHIP B R	TCGTGGACCGATCCAAACAG
CEP3 CHIP A F	GAGGACCCAACCCATCTTCATC
CEP3 CHIP A R	ACACGTACGTCCATTCCCATTT
E2Fa CHIP B- F	TTGCAGAGAATTGTGATT
E2Fa CHIP B- R	GAGAATCCGATCATAGAC
NAC1_RT-qPCR FW	CTCCTCGAGGCCGTAAAACC
NAC1_RT-qPCR RV	AGACCCAGTCTTCCTTTGGAG

Actin F	GGTAACATTGTGCTCAGTGGTGG
Actin R	AACGACCTTAATCTTCATGCTGC

586 **Table S3.** List of primer used.

587

588

589 **REFERENCES**

590 Battistella C, Guiet R, Burri O, Seitz A, Escrig S, Knott GW, Meibom A, Klok HA. (2019) Cellular
591 Uptake and Intracellular Trafficking of Poly(N-(2-Hydroxypropyl) Methacrylamide).
592 Biomacromolecules. 20(1):231-242. doi: 10.1021/acs.biomac.8b01372.

593 Baumberger N, Ringli C, Keller B. (2001). The chimeric leucinerich repeat/extensin cell wall
594 protein LRX1 is required for root hair morphogenesis in Arabidopsis thaliana. *Genes &*
595 *Development* 15, 1128–1139
596 Baumberger N, Steiner M, Ryser U, Keller B, Ringli C. (2003). Synergistic interaction of the two
597 paralogous Arabidopsis genes LRX1 and LRX2 in cell wall formation during root hair
598 development. *Plant Journal* 35, 71–81
599 Becker, C., Senyuk, V.I., Shutov, A.D., Nong, V.H., Fischer, J., Horstmann, C., and Müntz, K.
600 (1997). Proteinase A, a storage globulin-degrading endopeptidase of vetch (Vicia sativa
601 L.) seeds, is not involved in early steps of storage-protein mobilization. Eur. J. Biochem.
602 248: 304–312
603 Beers, E.P., Woffenden, B.J., Zhao C. (2000). Plant proteolytic enzymes: possible role during
604 programmed cell death. Plant Mol. Biol. 44, 399–415.doi: 10.1023/A:1026556928624
605 Berger F, Linstead P, Dolan L, Haseloff J. (1998) Stomata patterning on the hypocotyl of
606 Arabidopsis thaliana is controlled by genes involved in the control of root epidermis
607 patterning. *Dev Biol.* 194(2):226-34. doi: 10.1006/dbio.1997.8836.
608 Bolte S, Cordelières FP. (2006) A guided tour into subcellular colocalization analysis in light
609 microscopy. J Microsc. 224(Pt 3):213-32. doi: 10.1111/j.1365-2818.2006.01706.x.
610 Borassi C, Sede AR, Mecchia MA, Salgado Salter JD, Marzol E, Muschietti JP, Estevez JM.
611 (2016) An update on cell surface proteins containing extensin-motifs. J Exp Bot.
612 67(2):477-87. doi: 10.1093/jxb/erv455
613 Cannon MC et al (2008) Self-assembly of the plant cell wall requires an extensin scaffold. Proc
614 Natl Acad Sci USA 105:2226–2231.doi:10.1073/pnas.0711980105
615 Chen X., Cheng J., Chen L., Zhang G., Huang, H., Zhang Y., Xu L. (2016) Auxin-independent *NAC*
616 Pathway Acts in Response to Explant-Specific Wounding and Promotes Root Tip
617 Emergence during *De Novo* Root Organogenesis in *Arabidopsis*. Plant Physiol.
618 DOI:10.1104/pp.15.01733
619 Cheng Z, Guo X, Zhang J, Liu Y, Wang B, Li H, Lu H. (2020) βVPE is involved in tapetal
620 degradation and pollen development by activating proprotease maturation in
621 Arabidopsis thaliana. J Exp Bot. 25;71(6):1943-1955. doi: 10.1093/jxb/erz560
622 Fabrice T, Vogler H, Draeger C, Munglani G, Gupta S, Herger A, Knox P, Grossniklaus U,
623 Ringli C. (2018). LRX Proteins play a crucial role in pollen grain and pollen tube cell wall
624 development. *Plant Physiology* 176: 1981–1992
625 Grebe M, Xu J, Möbius W, Ueda T, Nakano A, Geuze HJ, Rook MB, Scheres B. (2003)
626 Arabidopsis sterol endocytosis involves actin-mediated trafficking via ARA6-positive
627 early endosomes. Curr Biol. 13(16):1378-87. doi: 10.1016/s0960-9822(03)00538-4.
628 Greenwood JS, Helm M, Gietl C (2005) Ricinosomes and endosperm transfer cell structure in
629 programmed cell death of the nucellus during Ricinus seed development. Proc Natl Acad
630 Sci USA 102:2238–2243. doi:10.1073/pnas.0409429102
631 Grierson C, Nielsen E, Ketelaarc T, Schiefelbein J. Root hairs. (2014) Arabidopsis Book.
632 12:e0172. doi: 10.1199/tab.0172.

633 Hall Q, Cannon MC. (2002) The cell wall hydroxyproline-rich glycoprotein RSH is essential for
634 normal embryo development in Arabidopsis. Plant Cell. 14(5):1161-72. doi:
635 10.1105/tpc.010477
636 He, X., and Kermode, A.R. (2003). Proteases associated with programmed cell death of
637 megagametophyte cells after germination of white spruce (Picea glauca) seeds. Plant
638 Mol. Biol. 52: 729–744
639 Helm M et al (2008) KDEL-tailed cysteine endopeptidases involved in programmed cell death,
640 intercalation of new cells, and dismantling of extensin scaffolds. Am. J. Bot. 95:1049–
641 1062. doi:10.3732/ajb.2007404
642 Hierl G, Vothknecht U, Gietl C (2012) Programmed cell death in *Ricinus* and *Arabidopsis*: the
643 function of KDEL cysteine peptidases in development. Physiol Plant 145:103–113.
644 doi:10.1111/j.1399-3054.2012.01580.x
645 Hierl G, Howing T, Isono E, Lottspeich F, Gietl C (2014) Ex vivo processing for maturation of
646 Arabidopsis KDEL-tailed cysteine endopeptidase 2 (AtCEP2) pro-enzyme and its storage
647 in endoplasmic reticulum derived organelles. Plant Mol Biol 84:605–620.
648 doi:10.1007/s11103-013-0157-6
649 Howing T, Huesmann C, Hoefle C, Nagel MK, Isono E, Huckelhoven R, Gietl C (2014)
650 Endoplasmic reticulum KDEL-tailed cysteine endopeptidase 1 of Arabidopsis (AtCEP1) is
651 involved in pathogen defense. Front Plant Sci 5:58. doi:10.3389/fpls.2014. 00058
652 Howing T, Dann M, Muller B, Helm M, Scholz S, Schneitz K, et al. (2018) The role of KDEL-
653 tailed cysteine endopeptidases of Arabidopsis (AtCEP2 and AtCEP1) in root
654 development. PLoS ONE 13(12): e0209407.
655 https://doi.org/10.1371/journal.pone.0209407
656 Jackson, P.A., Galinha, C.I., Pereira, C.S., Fortunato, A., Soares, N.C., Amâncio, S.B., and Pinto
657 Ricardo, C.P. (2001). Rapid deposition of extensin during the elicitation of grapevine
658 callus cultures is specifically catalyzed by a 40-kilodalton peroxidase. *Plant Physiol.* 127:
659 1065–1076
660 Maher KA, Bajic M, Kajala K, Reynoso M et al. (2018) Profiling of Accessible Chromatin Regions
661 across Multiple Plant Species and Cell Types Reveals Common Gene Regulatory
662 Principles and New Control Modules. *Plant Cell* 30(1):15-36.
663 Manders EMM, Verbeek FJ, Aten JA. (1993) Measurement of co-localization of objects in dual-
664 colour confocal images. *J Microsc*. 169(3):375-382. doi: 10.1111/j.1365-
665 2818.1993.tb03313.x.
666 Martinez-Pacheco J, Ranocha P, Kasulin L, Fusari CM, et al. (2022) Apoplastic class III
667 peroxidases PRX62 and PRX69 promote Arabidopsis root hair growth at low
668 temperature. Nat Commun. 14;13(1):1310. doi: 10.1038/s41467-022-28833-4
669 Marzol E, Borassi C, Bringas M, Sede A, Rodríguez Garcia DR, Capece L, Estevez JM. (2018).
670 Filling the Gaps to Solve the Extensin Puzzle. *Mol Plant*. 11(5):645-658
671 Marzol E, Borassi C, Carignani Sardoy M, Ranocha P et al. (2022) Class III Peroxidases PRX01,
672 PRX44, and PRX73 Control Root Hair Growth in *Arabidopsis thaliana*. Int J Mol Sci.
673 11;23(10):5375. doi: 10.3390/ijms23105375
674 Merkouropoulos G, Shirsat AH. (2003) The unusual Arabidopsis extensin gene atExt1 is
675 expressed throughout plant development and is induced by a variety of biotic and
676 abiotic stresses. Planta. 217(3):356-66. doi: 10.1007/s00425-003-1002-y
677 Ndinyanka Fabrice T, Kaech A, Barmettler G, Eichenberger C, Knox JP, Grossniklaus U, Ringli C
678 (2017) Efficient preparation of Arabidopsis pollen tubes for ultrastructural analysis using
679 chemical and cryo-fixation. BMC Plant Biol 17: 176

680 Olvera-Carrillo Y et al (2015) A conserved core of programmed cell death indicator genes
681 discriminates developmentally and environmentally induced programmed cell death in
682 plants. Plant Physiol 169:2684–2699. doi:10.1104/pp.15.00769
683 Ringli C. (2010). The hydroxyproline-rich glycoprotein domain of the Arabidopsis LRX1
684 requires Tyr for function but not for insolubilization in the cell wall. *Plant Journal* 63,
685 662–669
686 Sede AR, Borassi C, Wengier DL, Mecchia MA, Estevez JM, Muschietti JP (2018) Arabidopsis
687 pollen extensins LRX are required for cell wall integrity during pollen tube growth. FEBS
688 Lett 592:233-243
689 Schmid M, Simpson D, Gietl C (1999) Programmed cell death in castor bean endosperm is
690 associated with the accumulation and release of a cysteine endopeptidase from
691 ricinosomes. Proc Natl Acad Sci USA 96:14159–14164. doi:10.1073/pnas.96.24.14159
692 Schmid M, Simpson DJ, Sarioglu H, Lottspeich F, Gietl C (2001) The ricinosomes of senescing
693 plant tissue bud from the endoplasmic reticulum. Proc Natl Acad Sci USA 98:5353–5358.
694 doi:10.1073 /pnas.061038298
695 Schnabelrauch LS, Kieliszewski M, Upham BL, Alizedeh H, Lamport DT. (1996) Isolation of pl
696 4.6 extensin peroxidase from tomato cell suspension cultures and identification of Val-
697 Tyr-Lys as putative intermolecular cross-link site. Plant J. 9(4):477-89. doi:
698 10.1046/j.1365-313x.1996.09040477.x.
699 Showalter AM, Keppler B, Lichtenberg J, Gu D, Welch LR. (2010). A bioinformatics approach to
700 the identification, classification, and analysis of hydroxyproline-rich glycoproteins. Plant
701 physiology 153, 485–513
702 Strasser, R. (2016). Plant protein glycosylation. Glycobioogy 1014. doi:
703 10.1093/glycob/cww023
704 Su W, Liu Y, Xia Y, Hong Z, Li J. (2012). The Arabidopsis homolog of the mammalian OS-9
705 protein plays a key role in the endoplasmic reticulum associated degradation of
706 misfolded receptor-like kinases. Mol Plant. 5:929–940
707 Su W, Liu Y, Xia Y, Hong Z, Li J. (2011). Conserved endoplasmic reticulum-associated
708 degradation system to eliminate mutated receptor-like kinases in Arabidopsis. Proc Natl
709 Acad Sci USA. 108:870–875
710 Tanaka, T., Yamauchi, D., and Minamikawa, T. (1991). Nucleotide sequence of cDNA for an
711 endopeptidase (EP-C1) from pods of maturing Phaseolus vulgaris fruits. Plant Mol. Biol.
712 16: 1083–1084
713 Than ME, Helm M, Simpson DJ, Lottspeich F, Huber R, Gietl C (2004) The 2.0 A crystal
714 structure and substrate specificity of the KDEL-tailed cysteine endopeptidase
715 functioning in programmed cell death of Ricinus communis endosperm. J Mol Biol
716 336:1103–1116. doi:10.1016/j.jmb.2003.12.075
717 Velasquez SM, Ricardi MM, Dorosz JG, *et al*. (2011). O-Glycosylated Cell Wall Proteins Are
718 Essential in Root Hair Growth. Science 332, 1401–1403.
719 Velasquez SM, Marzol E, Borassi C, Pol-Fachin L, Ricardi MM, et al. (2015). Low sugar is not
720 always good: Impact of specific O-glycan defects on tip growth in Arabidopsis. Plant
721 physiology 168, 808–813
722 Velasquez M, Salter JS, Dorosz JG, Petersen BL, Estevez JM. (2012). Recent advances on the
723 posttranslational modifications of EXTs and their roles in plant cell walls. Frontiers in
724 plant science 3, 93

725 Wang, X., Wang, K., Yin, G., Liu, X., Liu, M., Cao, N., Duan, Y., Gao, H., Wang, W., Ge, W., et al.
726 (2018). Pollen-expressed leucine-rich repeat extensins are essential for pollen
727 germination and growth. *Plant Physiol*. 176, 1993–2006
728 Xie Q, Frugis G, Colgan D, Chua NH (2000) Arabidopsis NAC1 transduces auxin signal
729 downstream of TIR1 to promote lateral root development. Genes Dev 14: 3024–3036
730 Xie C, Li C, Wang F, Zhang F, Liu J, Wang J, Zhang X, Kong X, Ding Z. (2023) NAC1 regulates root
731 ground tissue maturation through coordinating with SCR/SHR-CYCD6;1 module in
732 Arabidopsis. Mol Plant. S1674-2052(23)00039-4. doi: 10.1016/j.molp.2023.02.006.
733 Zhang D et al (2014) The cysteine protease AtCEP1, a key executor involved in tapetal
734 programmed cell death, regulates pollen development in Arabidopsis. Plant Cell
735 26:2939–2961. doi:10.1105/tpc.114.127282
736 Zhou L-Z, Howing, T., Muller B., Hammes U.Z, Gietl C., Dresselhaus T. (2016) Expression
737 analysis of KDEL-CysEPs programmed cell death markers during reproduction in
738 Arabidopsis. Plant Reprod DOI 10.1007/s00497-016-0288-4
739 Zuo J, Niu QW, Chua NH (2000) Technical advance: An estrogen receptor-based transactivator
740 XVE mediates highly inducible gene expression in transgenic plants. Plant J. 24: 265-273

Parsed Citations

Battistella C, Guiet R, Burri O, Seitz A, Escrig S, Knott GW, Meibom A, Klok HA. (2019) Cellular Uptake and Intracellular Trafficking of Poly(N-(2-Hydroxypropyl) Methacrylamide). Biomacromolecules. 20(1):231-242. doi: 10.1021/acs.biomac.8b01372.
Google Scholar: Author Only Title Only Author and Title

Baumberger N, Ringli C, Keller B. (2001). The chimeric leucinerich repeat/extensin cell wall protein LRX1 is required for root hair morphogenesis in Arabidopsis thaliana. Genes & Development 15, 1128–1139
Google Scholar: Author Only Title Only Author and Title

Baumberger N, Steiner M, Ryser U, Keller B, Ringli C. (2003). Synergistic interaction of the two paralogous Arabidopsis genes LRX1 and LRX2 in cell wall formation during root hair development. Plant Journal 35, 71–81
Google Scholar: Author Only Title Only Author and Title

Becker, C., Senyuk, V.I., Shutov, A.D., Nong, V.H., Fischer, J., Horstmann, C., and Müntz, K. (1997). Proteinase A, a storage globulin-degrading endopeptidase of vetch (Vicia sativa L.) seeds, is not involved in early steps of storage-protein mobilization. Eur. J. Biochem. 248: 304–312
Google Scholar: Author Only Title Only Author and Title

Beers, E.P., Woffenden, B.J., Zhao C. (2000). Plant proteolytic enzymes: possible role during programmed cell death. Plant Mol. Biol. 44, 399–415.doi: 10.1023/A:1026556928624
Google Scholar: Author Only Title Only Author and Title

Berger F, Linstead P, Dolan L, Haseloff J. (1998) Stomata patterning on the hypocotyl of Arabidopsis thaliana is controlled by genes involved in the control of root epidermis patterning. Dev Biol. 194(2):226-34. doi: 10.1006/dbio.1997.8836.
Google Scholar: Author Only Title Only Author and Title

Bolte S, Cordelières FP. (2006) A guided tour into subcellular colocalization analysis in light microscopy. J Microsc. 224(Pt 3):213-32. doi: 10.1111/j.1365-2818.2006.01706.x.
Google Scholar: Author Only Title Only Author and Title

Borassi C, Sede AR, Mecchia MA, Salgado Salter JD, Marzol E, Muschietti JP, Estevez JM. (2016) An update on cell surface proteins containing extensin-motifs. J Exp Bot. 67(2):477-87. doi: 10.1093/jxb/erv455
Google Scholar: Author Only Title Only Author and Title

Cannon MC et al (2008) Self-assembly of the plant cell wall requires an extensin scaffold. Proc Natl Acad Sci USA 105:2226–2231.doi:10.1073/pnas.0711980105
Google Scholar: Author Only Title Only Author and Title

Chen X., Cheng J., Chen L., Zhang G., Huang, H., Zhang Y., Xu L. (2016) Auxin-independent NAC Pathway Acts in Response to Explant-Specific Wounding and Promotes Root Tip Emergence during De Novo Root Organogenesis in Arabidopsis. Plant Physiol. DOI:10.1104/pp.15.01733
Google Scholar: Author Only Title Only Author and Title

Cheng Z, Guo X, Zhang J, Liu Y, Wang B, Li H, Lu H. (2020) βVPE is involved in tapetal degradation and pollen development by activating proprotease maturation in Arabidopsis thaliana. J Exp Bot. 25;71(6):1943-1955. doi: 10.1093/jxb/erz560
Google Scholar: Author Only Title Only Author and Title

Fabrice T, Vogler H, Draeger C, Munglani G, Gupta S, Herger A, Knox P, Grossniklaus U, Ringli C. (2018). LRX Proteins play a crucial role in pollen grain and pollen tube cell wall development. Plant Physiology 176: 1981–1992
Google Scholar: Author Only Title Only Author and Title

Grebe M, Xu J, Möbius W, Ueda T, Nakano A, Geuze HJ, Rook MB, Scheres B. (2003) Arabidopsis sterol endocytosis involves actin-mediated trafficking via ARA6-positive early endosomes. Curr Biol. 13(16):1378-87. doi: 10.1016/s0960-9822(03)00538-4.
Google Scholar: Author Only Title Only Author and Title

Greenwood JS, Helm M, Gietl C (2005) Ricinosomes and endosperm transfer cell structure in programmed cell death of the nucellus during Ricinus seed development. Proc Natl Acad Sci USA 102:2238–2243. doi:10.1073/pnas.0409429102
Google Scholar: Author Only Title Only Author and Title

Grierson C, Nielsen E, Ketelaarc T, Schiefelbein J. Root hairs. (2014) Arabidopsis Book. 12:e0172. doi: 10.1199/tab.0172.
Google Scholar: Author Only Title Only Author and Title

Hall Q, Cannon MC. (2002) The cell wall hydroxyproline-rich glycoprotein RSH is essential for normal embryo development in Arabidopsis. Plant Cell. 14(5):1161-72. doi: 10.1105/tpc.010477
Google Scholar: Author Only Title Only Author and Title

He, X., and Kermode, A.R. (2003). Proteases associated with programmed cell death of megagametophyte cells after germination of white spruce (Picea glauca) seeds. Plant Mol. Biol. 52: 729–744
Google Scholar: Author Only Title Only Author and Title

Helm M et al (2008) KDEL-tailed cysteine endopeptidases involved in programmed cell death, intercalation of new cells, and dismantling of extensin scaffolds. Am. J. Bot. 95:1049–1062. doi:10.3732/ajb.2007404
Google Scholar: Author Only Title Only Author and Title

Hierl G, Vothknecht U, Gietl C (2012) Programmed cell death in Ricinus and Arabidopsis: the function of KDEL cysteine peptidases in development. Physiol Plant 145:103–113. doi:10.1111/j.1399-3054.2012.01580.x
Google Scholar: Author Only Title Only Author and Title

Hierl G, Howing T, Isono E, Lottspeich F, Gietl C (2014) Ex vivo processing for maturation of Arabidopsis KDEL-tailed cysteine endopeptidase 2 (AtCEP2) pro-enzyme and its storage in endoplasmic reticulum derived organelles. Plant Mol Biol 84:605–620. doi:10.1007/s11103-013-0157-6
Google Scholar: Author Only Title Only Author and Title

Howing T, Huesmann C, Hoefle C, Nagel MK, Isono E, Huckelhoven R, Gietl C (2014) Endoplasmic reticulum KDEL-tailed cysteine endopeptidase 1 of Arabidopsis (AtCEP1) is involved in pathogen defense. Front Plant Sci 5:58. doi:10.3389/fpls.2014. 00058
Google Scholar: Author Only Title Only Author and Title

Howing T, Dann M, Muller B, Helm M, Scholz S, Schneitz K, et al. (2018) The role of KDEL-tailed cysteine endopeptidases of Arabidopsis (AtCEP2 and AtCEP1) in root development. PLoS ONE 13(12): e0209407. https://doi.org/10.1371/journal.pone.0209407
Google Scholar: Author Only Title Only Author and Title

Jackson, P.A., Galinha, C.I., Pereira, C.S., Fortunato, A., Soares, N.C., Amâncio, S.B., and Pinto Ricardo, C.P. (2001). Rapid deposition of extensin during the elicitation of grapevine callus cultures is specifically catalyzed by a 40-kilodalton peroxidase. Plant Physiol. 127: 1065–1076
Google Scholar: Author Only Title Only Author and Title

Maher KA, Bajic M, Kajala K, Reynoso M et al. (2018) Profiling of Accessible Chromatin Regions across Multiple Plant Species and Cell Types Reveals Common Gene Regulatory Principles and New Control Modules. Plant Cell 30(1):15-36.
Google Scholar: Author Only Title Only Author and Title

Manders EMM, Verbeek FJ, Aten JA. (1993) Measurement of co-localization of objects in dual-colour confocal images. J Microsc. 169(3):375-382. doi: 10.1111/j.1365-2818.1993.tb03313.x.
Google Scholar: Author Only Title Only Author and Title

Martinez-Pacheco J, Ranocha P, Kasulin L, Fusari CM, et al. (2022) Apoplastic class III peroxidases PRX62 and PRX69 promote Arabidopsis root hair growth at low temperature. Nat Commun. 14;13(1):1310. doi: 10.1038/s41467-022-28833-4
Google Scholar: Author Only Title Only Author and Title

Marzol E, Borassi C, Bringas M, Sede A, Rodríguez Garcia DR, Capece L, Estevez JM. (2018). Filling the Gaps to Solve the Extensin Puzzle. Mol Plant. 11(5):645-658
Google Scholar: Author Only Title Only Author and Title

Marzol E, Borassi C, Carignani Sardoy M, Ranocha P et al. (2022) Class III Peroxidases PRX01, PRX44, and PRX73 Control Root Hair Growth in Arabidopsis thaliana. Int J Mol Sci. 11;23(10):5375. doi: 10.3390/ijms23105375
Google Scholar: Author Only Title Only Author and Title

Merkouropoulos G, Shirsat AH. (2003) The unusual Arabidopsis extensin gene atExt1 is expressed throughout plant development and is induced by a variety of biotic and abiotic stresses. Planta. 217(3):356-66. doi: 10.1007/s00425-003-1002-y
Google Scholar: Author Only Title Only Author and Title

Ndinyanka Fabrice T, Kaech A, Barmettler G, Eichenberger C, Knox JP, Grossniklaus U, Ringli C (2017) Efficient preparation of Arabidopsis pollen tubes for ultrastructural analysis using chemical and cryo-fixation. BMC Plant Biol 17: 176
Google Scholar: Author Only Title Only Author and Title

Olvera-Carrillo Y et al (2015) A conserved core of programmed cell death indicator genes discriminates developmentally and environmentally induced programmed cell death in plants. Plant Physiol 169:2684–2699. doi:10.1104/pp.15.00769
Google Scholar: Author Only Title Only Author and Title

Ringli C. (2010). The hydroxyproline-rich glycoprotein domain of the Arabidopsis LRX1 requires Tyr for function but not for insolubilization in the cell wall. Plant Journal 63, 662–669
Google Scholar: Author Only Title Only Author and Title

Sede AR, Borassi C, Wengier DL, Mecchia MA, Estevez JM, Muschietti JP (2018) Arabidopsis pollen extensins LRX are required for cell wall integrity during pollen tube growth. FEBS Lett 592:233-243
Google Scholar: Author Only Title Only Author and Title

Schmid M, Simpson D, Gietl C (1999) Programmed cell death in castor bean endosperm is associated with the accumulation and release of a cysteine endopeptidase from ricinosomes. Proc Natl Acad Sci USA 96:14159–14164. doi:10.1073/pnas.96.24.14159
Google Scholar: Author Only Title Only Author and Title

Schmid M, Simpson DJ, Sarioglu H, Lottspeich F, Gietl C (2001) The ricinosomes of senescing plant tissue bud from the endoplasmic reticulum. Proc Natl Acad Sci USA 98:5353–5358. doi:10.1073 /pnas.061038298
Google Scholar: Author Only Title Only Author and Title

Schnabelrauch LS, Kieliszewski M, Upham BL, Alizedeh H, Lamport DT. (1996) Isolation of pI 4.6 extensin peroxidase from tomato cell suspension cultures and identification of Val-Tyr-Lys as putative intermolecular cross-link site. Plant J. 9(4):477-89. doi: 10.1046/j.1365-313x.1996.09040477.x.
Google Scholar: Author Only Title Only Author and Title

Showalter AM, Keppler B, Lichtenberg J, Gu D, Welch LR. (2010). A bioinformatics approach to the identification, classification, and analysis of hydroxyproline-rich glycoproteins. Plant physiology 153, 485–513
Google Scholar: Author Only Title Only Author and Title

Strasser, R. (2016). Plant protein glycosylation. Glycobioogy 1014. doi: 10.1093/glycob/cww023
Google Scholar: Author Only Title Only Author and Title

Su W, Liu Y, Xia Y, Hong Z, Li J. (2012). The Arabidopsis homolog of the mammalian OS-9 protein plays a key role in the endoplasmic reticulum associated degradation of misfolded receptor-like kinases. Mol Plant. 5:929–940
Google Scholar: Author Only Title Only Author and Title

Su W, Liu Y, Xia Y, Hong Z, Li J. (2011). Conserved endoplasmic reticulum-associated degradation system to eliminate mutated receptor-like kinases in Arabidopsis. Proc Natl Acad Sci USA. 108:870–875
Google Scholar: Author Only Title Only Author and Title

Tanaka, T., Yamauchi, D., and Minamikawa, T. (1991). Nucleotide sequence of cDNA for an endopeptidase (EP-C1) from pods of maturing Phaseolus vulgaris fruits. Plant Mol. Biol. 16: 1083–1084
Google Scholar: Author Only Title Only Author and Title

Than ME, Helm M, Simpson DJ, Lottspeich F, Huber R, Gietl C (2004) The 2.0 A crystal structure and substrate specificity of the KDEL-tailed cysteine endopeptidase functioning in programmed cell death of Ricinus communis endosperm. J Mol Biol 336:1103–1116. doi:10.1016/j.jmb.2003.12.075
Google Scholar: Author Only Title Only Author and Title

Velasquez SM, Ricardi MM, Dorosz JG, et al. (2011). O-Glycosylated Cell Wall Proteins Are Essential in Root Hair Growth. Science 332, 1401–1403.
Google Scholar: Author Only Title Only Author and Title

Velasquez SM, Marzol E, Borassi C, Pol-Fachin L, Ricardi MM, et al. (2015). Low sugar is not always good: Impact of specific O-glycan defects on tip growth in Arabidopsis. Plant physiology 168, 808–813
Google Scholar: Author Only Title Only Author and Title

Velasquez M, Salter JS, Dorosz JG, Petersen BL, Estevez JM. (2012). Recent advances on the posttranslational modifications of EXTs and their roles in plant cell walls. Frontiers in plant science 3, 93
Google Scholar: Author Only Title Only Author and Title

Wang, X., Wang, K., Yin, G., Liu, X., Liu, M., Cao, N., Duan, Y., Gao, H., Wang, W., Ge, W., et al. (2018). Pollen-expressed leucine-rich repeat extensins are essential for pollen germination and growth. Plant Physiol. 176, 1993–2006
Google Scholar: Author Only Title Only Author and Title

Xie Q, Frugis G, Colgan D, Chua NH (2000) Arabidopsis NAC1 transduces auxin signal downstream of TIR1 to promote lateral root development. Genes Dev 14: 3024–3036
Google Scholar: Author Only Title Only Author and Title

Xie C, Li C, Wang F, Zhang F, Liu J, Wang J, Zhang X, Kong X, Ding Z. (2023) NAC1 regulates root ground tissue maturation through coordinating with SCR/SHR-CYCD6;1 module in Arabidopsis. Mol Plant. S1674-2052(23)00039-4. doi: 10.1016/j.molp.2023.02.006.
Google Scholar: Author Only Title Only Author and Title

Zhang D et al (2014) The cysteine protease AtCEP1, a key executor involved in tapetal programmed cell death, regulates pollen development in Arabidopsis. Plant Cell 26:2939–2961. doi:10.1105/tpc.114.127282
Google Scholar: Author Only Title Only Author and Title

Zhou L-Z, Howing, T., Muller B., Hammes U.Z, Gietl C., Dresselhaus T. (2016) Expression analysis of KDEL-CysEPs programmed cell death markers during reproduction in Arabidopsis. Plant Reprod DOI 10.1007/s00497-016-0288-4
Google Scholar: Author Only Title Only Author and Title

Zuo J, Niu QW, Chua NH (2000) Technical advance: An estrogen receptor-based transactivator XVE mediates highly inducible gene expression in transgenic plants. Plant J. 24: 265-273
Google Scholar: Author Only Title Only Author and Title